POLITECNICO DI TORINO

Master degree course in Electronic Engineering

Master Degree Thesis

Team PoliTOcean

R.O.V. Prototypes and an Ultrasonic Underwater Triggering System

Supervisor
Prof. Claudio Sansoè

Candidate
Dario Gaetano Sciortino

Academic year 2018-2019

Summary

This thesis is mainly divided in two topics. The first regards the birth, growth and results of the students' team called *PoliTOcean*, while the second is about the design and development of an ultrasonic system for short range underwater communications.

Since my high school thesis was about the design and development of an R.O.V., I had the idea to start a new student team to introduce inside the university the topic of underwater robotics, for educational and research purposes. On chapter 1 it will be described what an R.O.V. is but, for the moment, let's assume it is an underwater drone.
The Professor C. Sansoè, already active in the context of underwater electronic in general, enthusiastically accepted to fill the role of supervisor of the team, that initially counted 11 students. On April 2017, the team was officially born with the approval by the university's commission.

Since then, and until September 2018, I covered inside the team the role of Team Leader and electronics developer. Two R.O.V. prototypes have been made and will be described here in chapter 2 and chapter 3, while another one is currently being designed.
One of the main technical challenges that I personally faced, was the development of an ultrasonic system to send a triggering signal , from the R.O.V to a submersed device, at a distance of some centimeters. This system will be described in detail on chapter 4.

Acknowledgements

The firsts and most heartfelt thanks goes to the family and especially to my mother, that raised me and my extraordinary two sisters Giulia and Chiara and my sweet nice Sofia. My whole family always encouraged me in everything I did, but I'm sure my cousin Luca pulled the trigger to my "geek" side since my boyhood.
What I'm writing about on this thesis would have never started, as many other things in my life, without the support and complicity of Hilde, my partner in every way.
I would like to thank my colleagues and "Turin's friends" Damiano, Federico, Giorgio, Giovanni, Lorenzo, Riccardo and Sebastiano, that allowed this studies to be cheerful. Of course my best friend Giovanni, even if distant, has always been here with the heart.
I feel that it's a fact that I wouldn't be the person that I feel to be without the Collegio R. Einaudi, that's way I could never end to say thank you to those people that I lived with during this years.

A big thank go to the professor and mentor Prof. C. Sansoè, that believed in the project since the first moment. More than anything, with an enviable patience, he helped us to fill that gap that was originally present between us students and the University as a public administration, teaching us how to deal with the bureaucratic affairs and advising us in the technical choises.
To conclude, a proper thank you goes to all the team members that participated and actually gave a real value to the team, they are too many to list but at least the co-founders need to be said: Antonio, Damiano, Detjon, Flavio, Francesco, Hilde, Massimo, Riccardo, Simone and Tommaso.
Massimo needs a special one, as always demonstrated his efforts and love to the team. He will now replace me as team leader of this group, and I'm sure he's been the most suited person to this role.

Contents

List of Tables

List of Figures

Chapter 1

Introduction to R.O.V.s

R.O.V. is an achronym that stands for Remotely Operated Vehicle. More properly, it should be R.O.U.V. standing for Remotely Operated Underwater Vehicle. It is indeed an unmanned and tethered underwater vechicle, usually piloted from a vessel, an offshore platform or even from a proximate land. They are always equipped with at least one camera that streams the video up to the surface in order to perform the operations.

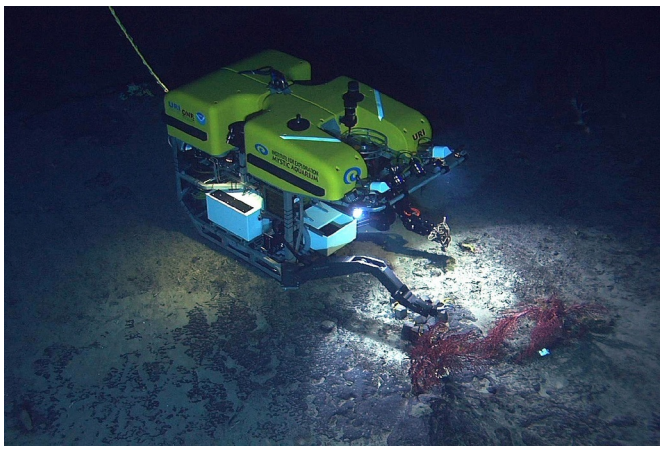

Figure 1.1: The Hercules ROV in action, for scientific research. Photo credit: NOAA photo library

The main field of application of this vehicles is usually offshore hydrocarbon platforms, for tasks such as submersed infrastructures maintenance and search. Of course, they are not limited to it and are widely used for scientific research, usually in the deepest parts of the oceans, as we can see in Figure 1.1.

They are usually divided into five main classes, defined as follows:

- **Class I** Usually called *Eyeballs*. They are relatively small R.O.V.s used for inspection purposes, typically equipped with a single camera and sometimes with an small manipulator. Their operative depth is usually around 300 m.
- **Class II** Can reach depths up to 3000 m and, contrary to the inspection ones, may need a special system for their deployment. Usually equipped with more than one camera, various sensors and a manipulator for light works like knobs handling.
- **Class III** Often called *Work class*, these are mainly used from oil or gas companies due to their high payload capabilities, such as scanning sensors for seabed mapping, and because of their high power that is mainly hydraulic. Their operative depth is up to 10000m.
- **Class IV** Called *Excavators*, only operates on the seabed for operations like the burial of pipelines. Hence, they are often provided with crawlers.
- **Class V** A.U.V.s (*Autonomous Underwater Vehicles*) belongs to this category. They differ from the other listed above since they do not have a tether that connects them to the surface. Thus, they need to be autonomous in some way and this is often translated into following a certain path to plumb the seafloor.

(a) Sirio: 40 kg (b) Pegaso: 350 kg

Figure 1.2: An example of Class I and III R.O.V.s by *Lightouse-geo*

1.1 Purposes of the team

As said before, the main purpose of the team is to introduce inside the university the topic of underwater robotics. It has been clear that the best approach to reach this goal would have been to build an R.O.V. prototype. The construction of a similar vehicle requires knowledge in all the main *STEM* subjects, and is thus fundamental to involve students from all the different university's courses.
As a consequence, the team results to be an optimal opportunity for every student to face new challenges and apply theoretical knowledge in a practical way.

Our main goal has been, and at the moment still is, the participation to the *MATE R.O.V.* competition. An annual international event, in which the best R.O.V. teams are selected to compete and perform some underwater tasks.
These tasks are often the simulation and simplification of possible real-context ones, like the handling and recovery of some objects, areas inspections or generic measurements.

Chapter 2

First R.O.V.

In this chapter will be described the main steps of the design and development of the first R.O.V. that the team built.
This prototype has been built between May and July 2017, with the only intention to expertise the team members and to build solid foundation from which the team could start, in the view of the participation to the *MATE R.O.V 2018* competition. The idea was then to build a simple one, that could essentially be defined as an underwater drone.

2.1 Mechanics

The mechanical realization of the vehicle was perhaps the step that may have taken a long time, so we decided to make it as simple as possible.

2.1.1 Chassis

The structure wouldn't have needed to handle any strong mechanical stress. Thus, we just had to cut PVC pipes, to be assembled through some 3D-printed joints. In Figure 2.1 there is a rendering of the mechanical structure only, before it was build. The numbers indicate:

1. Plexiglass waterproof tube, bought by *Bluerobotics*, that will host the electronics. On the front, there is a transparent interface while on the rear, there is a drilled flange in order to insert the penetrators (see section A.1) of the wires coming from the thrusters

2. PVC pipes of 25 mm diameter, which constitute the chassis

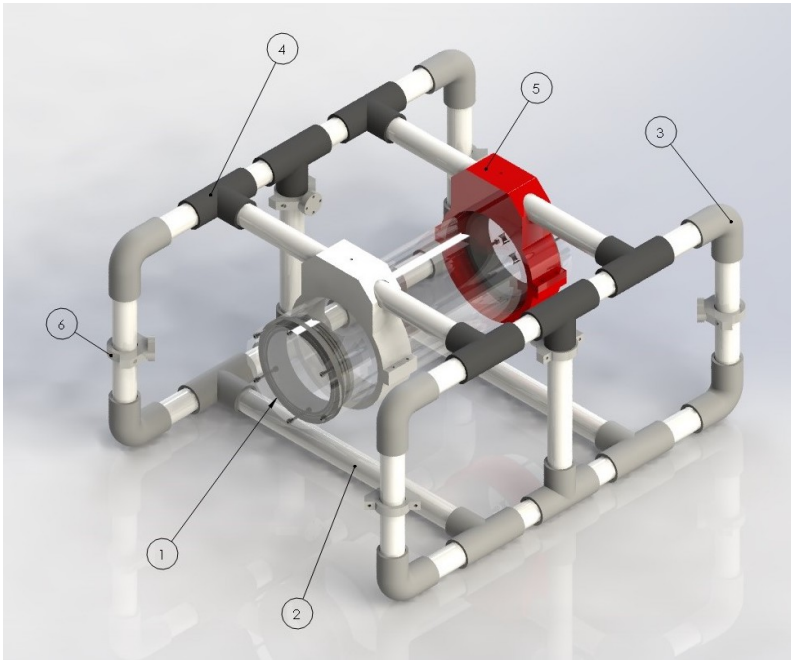

Figure 2.1: Mechanical structure of the first R.O.V. prototype. Photo credit: PoliTOcean mechanical team

3. "C" 3D printed joints, made in ABS
4. "T" 3D printed joints, made in ABS
5. Flange to attach the electronics enclosure to the chassis, still 3D-printed
6. 3D printed brackets, used to position the thrusters and possibly modify their orientation on the need

2.1.2 Thrusters

In order to decide the positioning of the thrusters, some priorities needed to be defined in order to reach a tradeoff.
Two possible solutions were discussed, both exploiting six thrusters in order to try to cover all the possible degrees of freedom such as *pithc, roll, yaw* and *heave, surge* and *sway*. This degrees of freedom, characteristics of the R.O.V.s can be understood thanks to Figure 2.2.

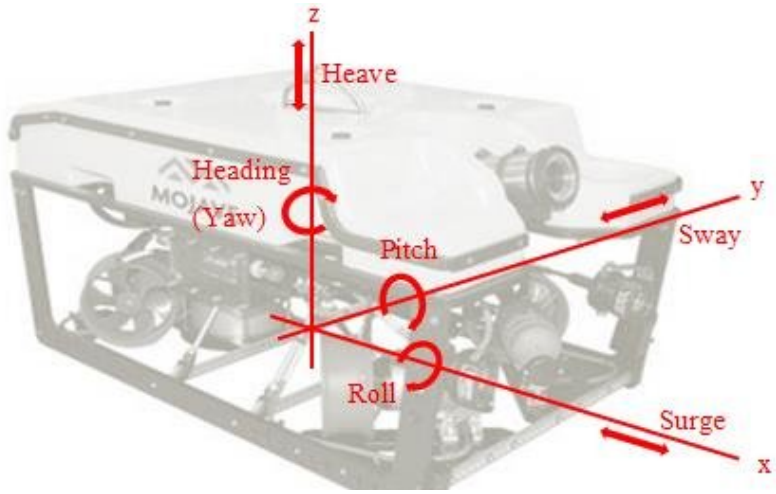

Figure 2.2: Image explaining the degrees of freedom of an R.O.V.. Photo credits: See [1]

Generally, R.O.V.s use at least three thrusters, in order to allow at least *heave, surge* and *yaw* control. Usually, one vertical and two horizontal like in some Class I R.O.V.s.
In some cases, when the *sway* is needed, at least one lateral thruster is used to allow this movement.
To enable all the six degrees of freedom, at least six thrusters must be utilised. Commercial solutions generally make use of two horizontal thrusters for *surge* and *yaw* control,one for *sway* as said before combined with at least three vertical ones controlling *roll*, *pitch* and *heave*.

The possible solution analyzed for our first approach will be described below, considering that one of the main priority was to use at most six thrusters and enable as much degrees of freedom as possible.

Two possible solutions were then discussed:

- **Solution 1**: This solution requires four horizontal motors to be placed along the vertical plane, and the other two along the horizontal one.
  In this way, all the possible degrees of freedom are covered: *pitch*, *roll* and *yaw* can be easily performed as in 2.3a, 2.3b, 2.3c. Moreover, *surge* and *heave* can be done without causing any particular side effect. The *sway*, instead, requires on this configuration to pilot the left and right part of the vertical thrusters in an opposite way, creating of necessity a *roll* toward the direction of the *sway*, as can be seen in 2.3f.

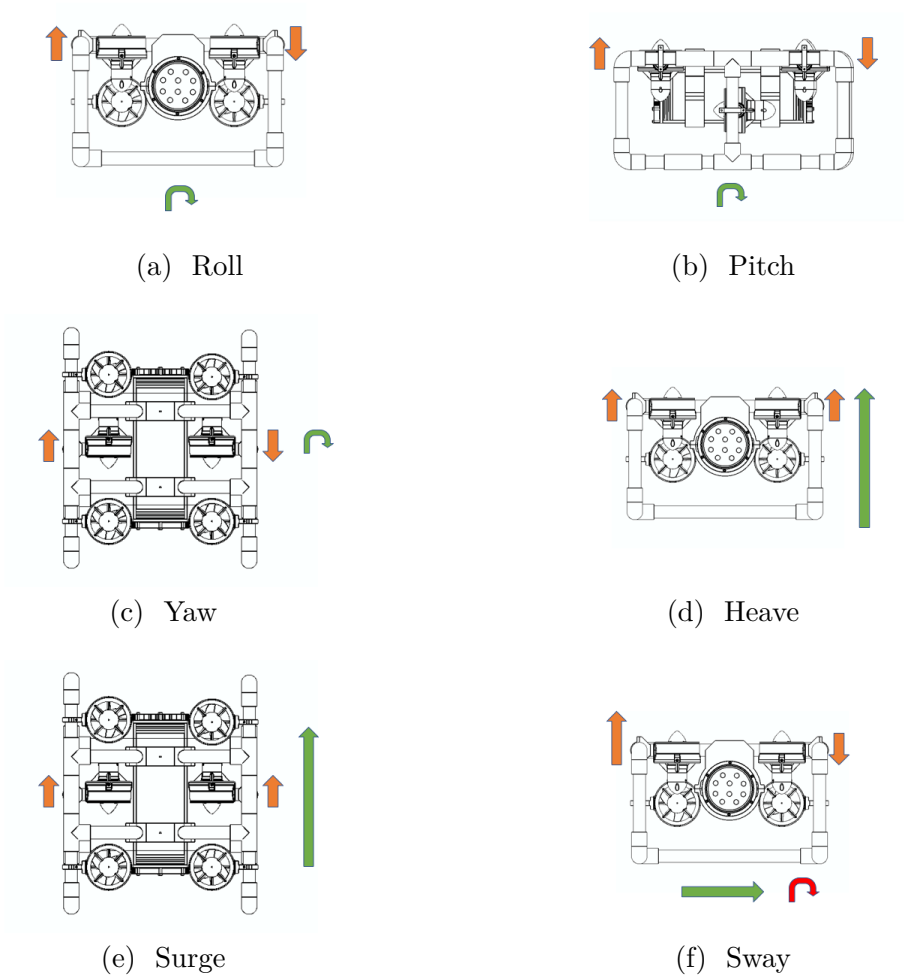

(a) Roll (b) Pitch

(c) Yaw (d) Heave

(e) Surge (f) Sway

Figure 2.3: Motor piloting for the movements. Orange arrows represent single motor thrusts, green ones the wanted effects and in red the side effects

- **Solution 2**: This solution requires two horizontal motors to be placed along the vertical plane, and the other four along the horizontal one, placed with 45° angles.
  In this way, the *sway* and the *surge* can be performed by means of the horizontal motors, without causing any particular side effect but of course being less efficient due to the angled positioning of them. The *heave* instead is done thanks to the two vertical thrusters.
  Yaw and *roll*, are also here performed easily bu the *pitch* results instead to be unfeasible as the two vertical motors cannot act to produce it.

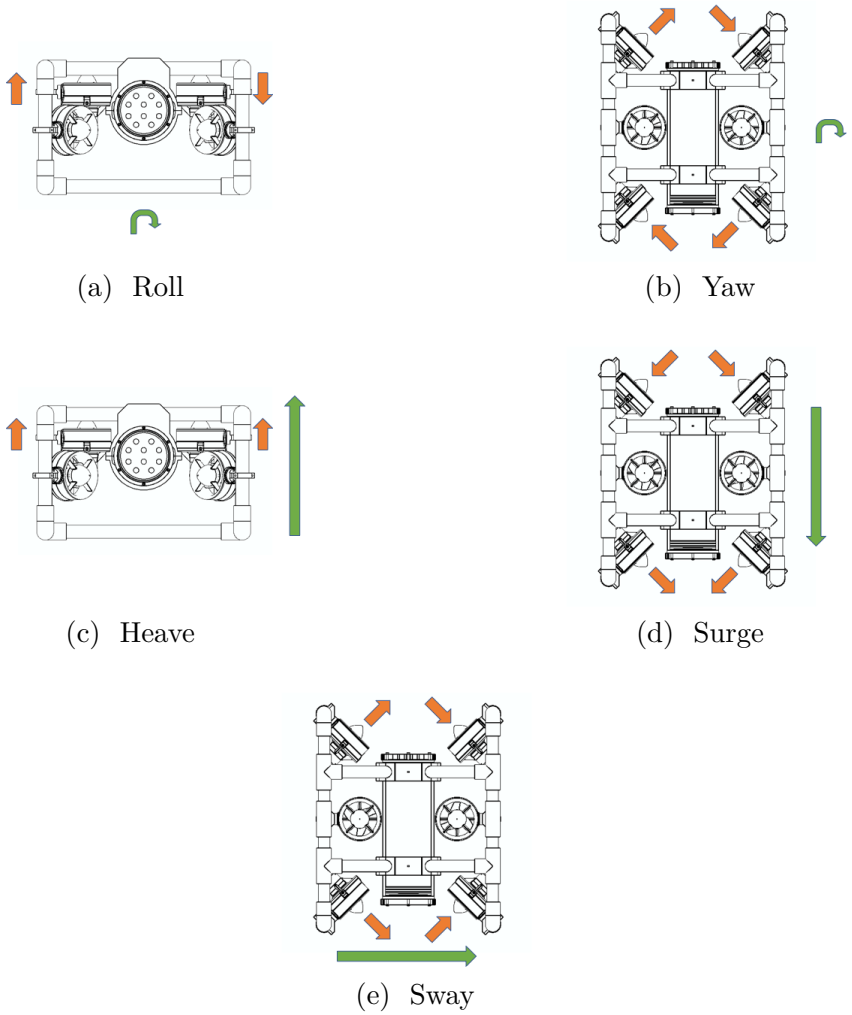

(a) Roll (b) Yaw

(c) Heave (d) Surge

(e) Sway

Figure 2.4: Motor piloting for the movements: notice that the pitch cannot be done

What comes out is that the first solution allows to cover all the possible degrees of freedoms, as long as the *roll* side effect on the *sway* is considered to be acceptable.
The second solution instead, allows the *sway* to be free of any side effect but does not allow to perform the *roll* and the efficiency of the thrusters along any horizontal movement is reduced.
It has been decided to adopt the first solution, mostly because having all the degrees of freedom would have allowed the students working on the software to have more to learn. Moreover, having four vertical thrusters available, an active controller on the horizontal plane could have been developed, in order to compensate possible *pitch* and *roll* unwanted movements due to mechanical imbalances or system disturbances.

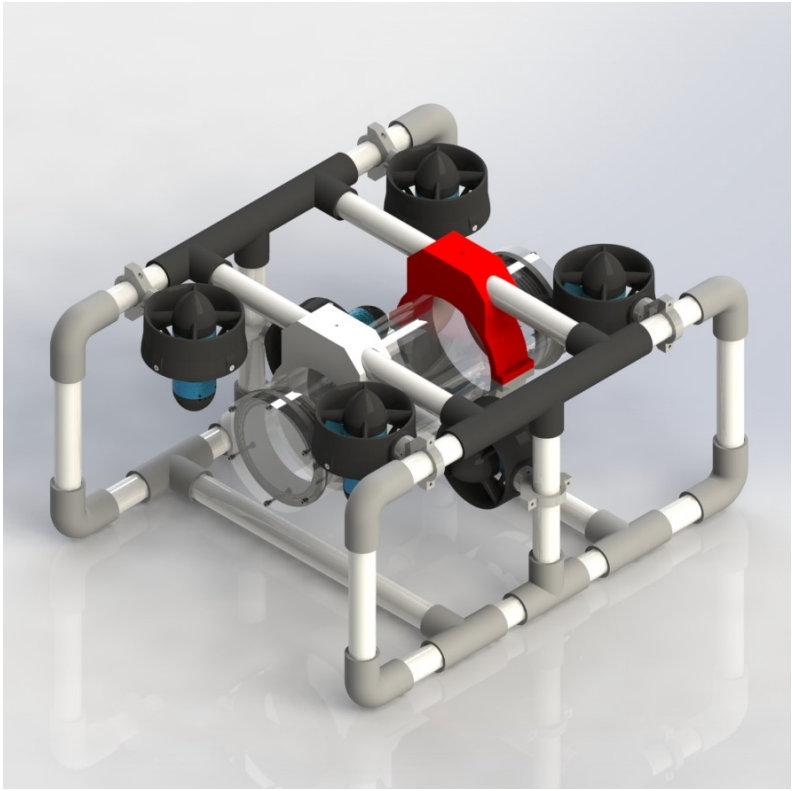

Figure 2.5: Rendering of the first R.O.V. prototype with 4 vertical motors and 2 horizontal ones. Photo credit: PoliTOcean mechanical team

The thrusters chosen for this purpose are the *T200* by Bluerobotics, as they result to be very efficient and the most documented underewater motors available on the market. Moreover, their cost is relatively low.

2.1.3 Electronics housing

The electronics housing had to host the PCBs only, as for this prototype version the camera and its video transmission was not a priority.
The *Bluerobotics* 4" acrylic tube bought for this purpose is rated to 100 m deep. The aluminium version of the same tube is instead rated for depths up to 600 m [2].
Thus, the electronics enclosure results to be in any case the bottleneck of the system, as the T200 thrusters have been successfully tested to be rated at least 3000 m [3].
Even if the acrylic tube is rated for depth much lower with respect with its aluminium corresponding one, it has been clear that for a first prototype would have been more important to monitor the internal conditions of the enclosure (notice possible leaks or led status) while in operation, rather than being capable of diving deeper.
Only one PCB, that will be described in the next section, needed to be hosted in the enclosure, but a mechanical system needed to be designed in order to hold it firmly inside the enclosure.
The resulting design is represented in Figure 2.6, whereas the grey discs are made of 3D-printed PLA.

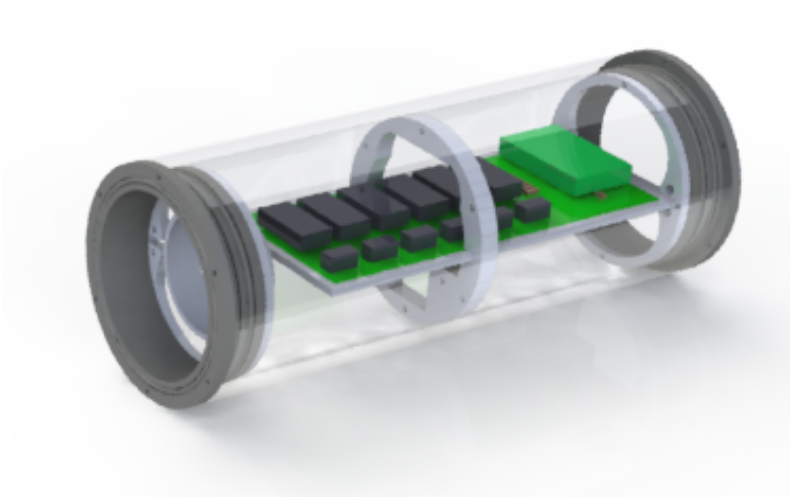

Figure 2.6: Rendering of the electronics enclosure. Photo credit: PoliTOcean mechanical team

As can be seen, an holding system for a possible camera has been designed as well, in order to place it in the front of the enclosure, even if at the end it was not used.

2.2 Electronics

The main requirements of the electronic was to control the six thrusters and to communicate with the surface.This has been accomplished by using one *ESC* (see section A.2) for each motor, that just needed a *PWM* signal to control it.
The communication protocol have been chosen to be the *RS-485*, because of its strength to external noise, easiness of implementation and the economy of the hardware. Moreover, an half-duplex communication was at that moment more than enough, since the main stream of data would have come from the surface control station just to impose the R.O.V. direction.
An *IMU* (see **??** has instead been used in order to compensate the movements.
Thus, the microcontroller resulted to only have as output the *ESCs*' *PWM* signal, and as an input the serial command sent from the surface to pilot the R.O.V..

2.2.1 Scheme and PCB

In Figure 2.7 are grouped the five main parts of the electronic to control the R.O.V.:

1. **Power**: Since by competition rules one of the most important requirements was to power the R.O.V with 48V, a conversion has been necessary for both the thrusters' power and the logical electronic one. A 48V to 12V DCDC *CHS5004812* has been used in order to efficiently convert the voltage for the motor, and a simple LDO voltage regulator *LM7805* has been used to power the logical electronics.

2. **Logic**: The microcontroller *ATmega328P* has been used in order to read the surface command, the *IMU* data and write the *PWM* signal to the the *ESCs*' input pins.
   This microcontroller resulted to be the most suitable as it is the one used by various models of *Arduino*. Thus, the simplicity in the flashing of the code, the availability of the huge number of libraries is made possible thanks to the community that is being developed around it.

3. **Inputs**: Here a *MAX485* is used in order to convert the half-duplex *RS-485* to a simpler TTL compatible one. An ethernet cable with a length of 30 m has been used as propagation medium. The *IMU* has

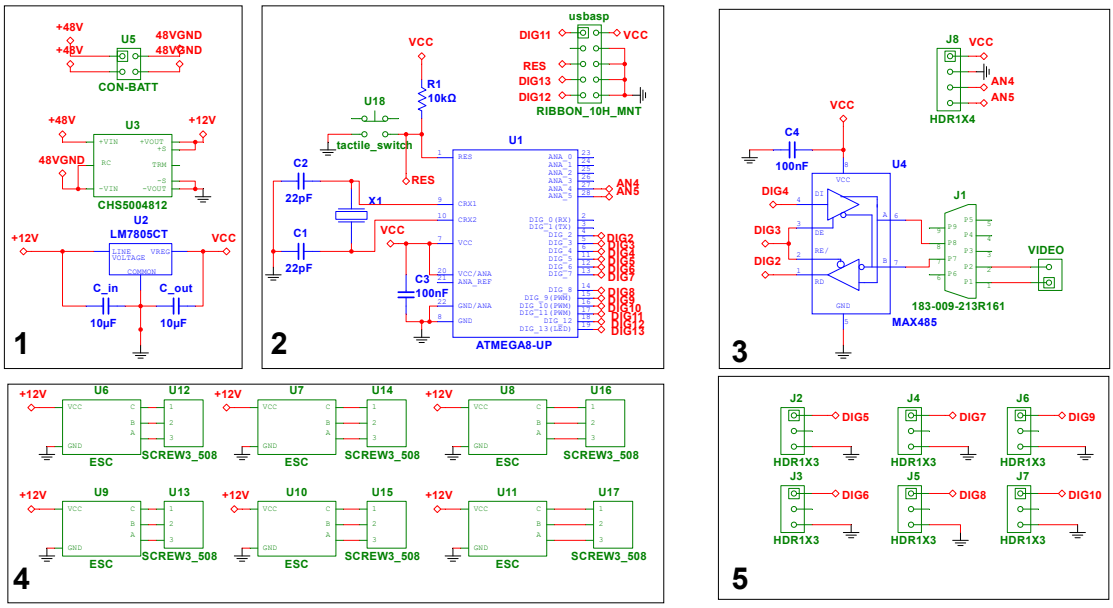

Figure 2.7: Scheme of the first R.O.V. PCB. Photo credit: PoliTOcean electronics team

instead been connected to the I^2C bus. This component has not been directly soldered to the PCB but rather connected by means of cables, since its optimal position is at the center of gravity of the R.O.V., whose position couldn't be determined a priori.

4. ***ESCs***: are directly powered from the PCB and its output goes to 3-ways screw connectors, to which the thrusters are connected once they enter the electronic enclosure by means of the penetrators.

5. **Signals** of the *ESCs*: are simple *PWM* signals generated from the microcotroller's GPIOs. This *PWM* values can go from 1100 to 1900 µs, to which the maximum reverse and forward thrust are generated respectively.
   At 12V, the maximum forward thrust is 3.55 kgf while the maximum reverse thrust is 3.00 kgf [4].

In Figure 2.8 can be seen that the top layer of the PCB has been used for the power components such as the DCDC converter and the six *ESCs*, with their screw terminals to be connected to the motors.
The bottom has been used to place the microcontroller and the remaining digital components.

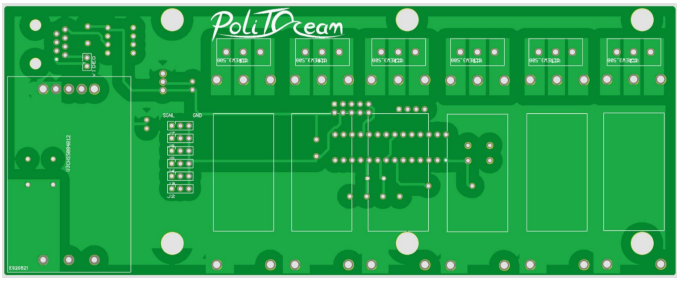

(a) Top view

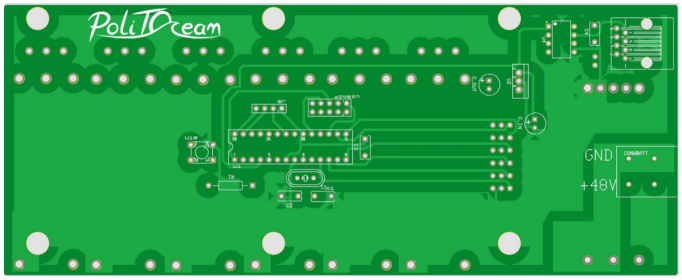

(b) Bottom view

Figure 2.8: A rendering of the PCB once the gerber files have been uploaded on a manufacturer website

2.3 Software

Once the *IMU* data are read and the orientation of the R.O.V. is determined [5], a proportional controller has been developed such that the R.O.V. automatically sets itself with null *pitch* and *roll* angles.
On the surface side, instead, the values of the axis of an USB Joystick are read thanks to a Python script and the library *Pygame*. This values are then encapsulated into a string that is sent, from the same script and thanks to the library *Serial*, to the R.O.V. by means of and USB/RS-485 converter.

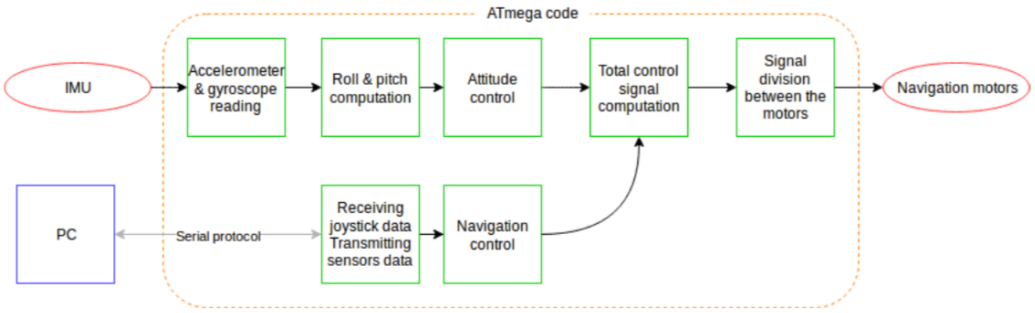

Figure 2.9: Scheme representing the code structure of the ATmega. Photo credit: PoliTOcean it team

In Figure 2.9 the main blocks of the algorithm implemented in the onboard microcontroller are described.

2.4 Features

The key characteristics of the resulting R.O.V. prototype, that can be seen in Figure 2.5 are the following:

- 48V 30A power supply
- 23.5x40x48cm (HxWxL), 5 kg in air without cable
- 100 m maximum depth
- 6 degrees of freedom
- Autostabilisation on the horizontal plane

The weakest component is the electronic acrylic enclosure and from here the maximum operative depth of 100 m. Of course, it can be easily increased by changing it with the aluminium one.

Chapter 3

Second R.O.V

As said in the previous chapter, the first vehicle allowed the team to develop a certain practical know-how and confidence on the R.O.V. world .
The second prototype has been designed and developed from November 2017 to June 2018, in order to participate to the *MATE R.O.V* Competition that has been held in Seattle (WA) on 20-22 June 2018.
In this chapter will follow an overview of the whole system. The name chosen for this R.O.V. is *Nereo*.

3.1 Main competition requirements

The 2018 competition was divided in three main tasks, to be undertaken within 15 minutes in a 5 meters deep pool, synthetized below.
Of course, all the referred items called *props* want just to simulate a real scenario and it is straightforward that their weight, dimensions and/or materials would not reflect a real one:

- **Aircrafts**: An aircraft engine (3.1a) has to be retrieved from the seafloor. In order to do so, the debris (3.1b) located on the top of it have first to be moved away by means of a liftbag (see section A.3) and leave them in a certain zone. At this point, the same liftbag (or another one) may be used in order to retrieve the engine to the surface.

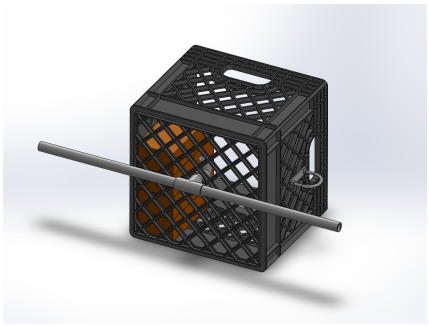

(a) Engine: 6 kg in water

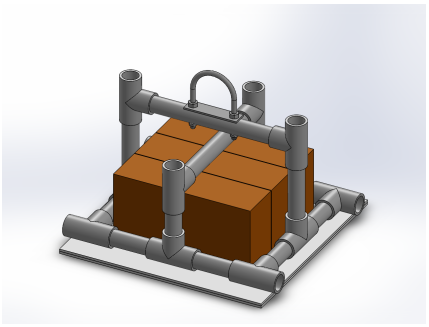

(b) Debris: 4 kg in water

Figure 3.1: A rendering of the *props* representing the engine and the debris on the top of it. Photo credit: MATE

- **Earthquakes**: This task essentially requires to level an *O.B.S.* (Ocean Bottom Sysmographer, Figure 3.2) by means of rotating the four handles on its corners, once it has been powered through the insertion of an inductive power connector.

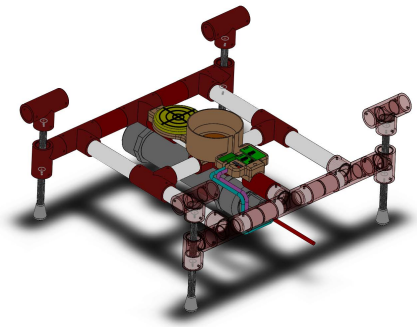

Figure 3.2: A rendering of the *prop* representing the O.B.S. . Photo credit: MATE

- **Energy**: Divided in many subtasks:
  - Install and lock, by means of a handle latching system, a tidal turbine array to its base (3.3a)
  - Install and lock an *I-AMP* (Intelligent Adaptable Monitoring Package, 3.3b) into its base by means of a sliding locking mechanism

– Place a mooring (3.3c) at a given distance from the tidal turbine array, then attach to its chain a velocimeter at a certain height

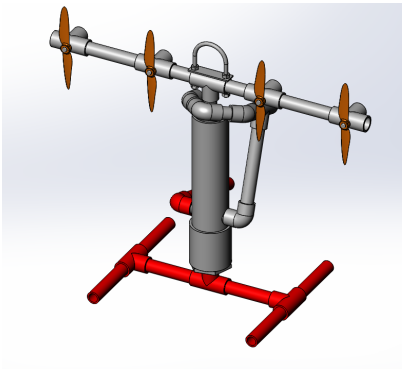

(a) Array of four turbines latched into its base

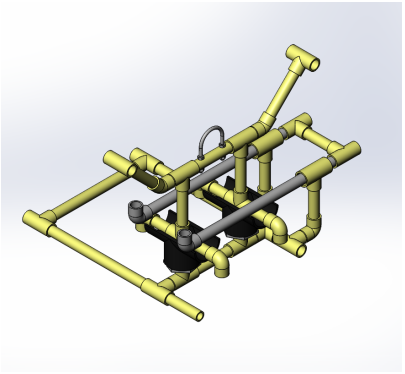

(b) I-AMP locked by the grey sliding mechanism

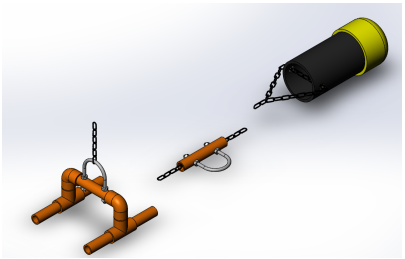

(c) Section of the mooring. From left to right: anchoring base, velocimeter attachment, floating buoy

Figure 3.3: A rendering of the *props* for the Energy tasks. Photo credit: MATE

The competition requirements of course implied many changes in our original structure that, as it was, it could not have afforded the tasks.
Moreover, with the previous prototype, we had the possibility to point out some must-have optimization in the designs of both the mechanical and electronic part. As an example: improve the stability of the structure, adding the possibility to translate the R.O.V. left and right along the horizontal plane without having a *roll*, allow an easier access to the electronic enclosure and many other aspects.

3.2 Mechanics

3.2.1 Robotic arm

First of all, a robotic arm was essential to all the three main sub-tasks. Thus, it has been one of the first points from which the design phase started. In particular, three degrees of freedom were needed and can be seen in Figure 3.4:

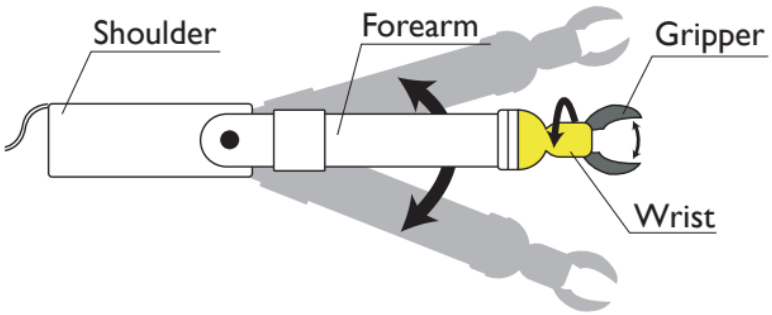

Figure 3.4: A simplified scheme of the robotic arm, with its degrees of freedom. Photo credit: PoliTOcean design team

- **Gripper**: in order to ensure not only a secure holding of the objects such as the liftbag or the O.B.S. handles, but also the possibility to grab and release objects on the need.
- **Wrist**: mainly needed by the O.B.S. task in order to rotate the handles, but revealed to be useful also for other operations that the pilot had to face, such as objects handling and positioning.
- **Shoulder**: allowed the pilot to rotate objects underneath the R.O.V., such as the O.B.S. handles, without having to perform any *pitch*.

In Figure 3.5 there is a rendering of the final arm that has been mounted on the R.O.V..
All the white components that can be seen, have been designed in order to be produced with a particular and sofisticated 3D-printing technique such as the stereolithography technology (*SLA*).This is an extremely precise 3D-printing process based on the photopolymerization, so that the material of the cases is a kind of waterproof resin, with performances similar to the ABS.
The yellow and black ones have been instead produced with a common 3D printer based on the fused deposition modeling technology (*FDM*). This technique results to be extremely cheaper with respect to the previous one, but does not guarantee any waterproofing and, in fact, it has been exploited only for those components that are not holding any electronic material ar motors.
The shoulder case is covered by a transparent acrylic plate, in order to point out eventual leaks.

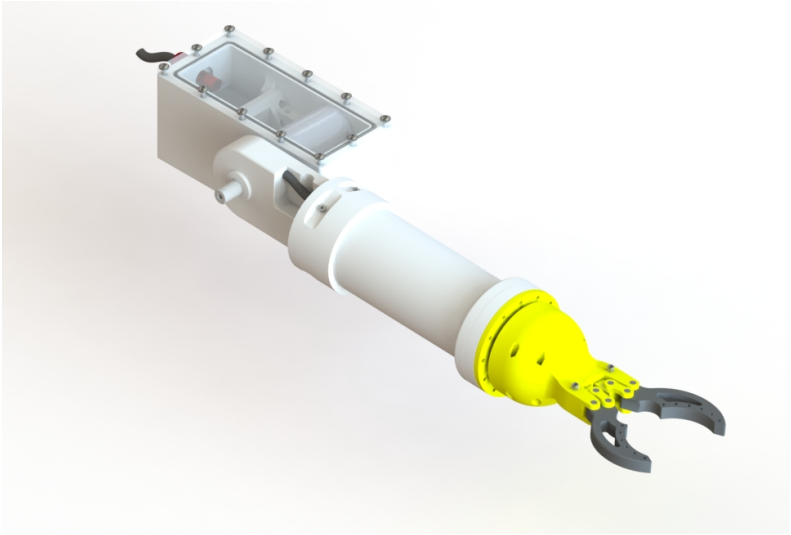

Figure 3.5: Rendering of the arm. Photo credit: PoliTOcean mechanical team

The different degrees of freedom have been reached thanks to two stepper motors and a linear actuator, located into the shoulder and forearm cases as described below:

- Inside the **shoulder** (3.6a), a *NEMA17* stepper motor is used in order to drive a worm-gear system. This mechanical configuration allows to transfer the motion in 90° degrees and to improve the torque as well.
  The movement results in the rotation of the shoulder in each direction

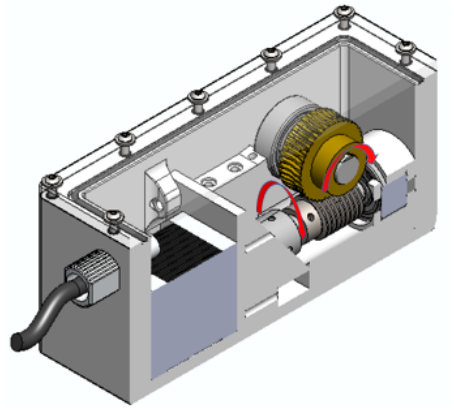

(a) Section of the forearm mechanism

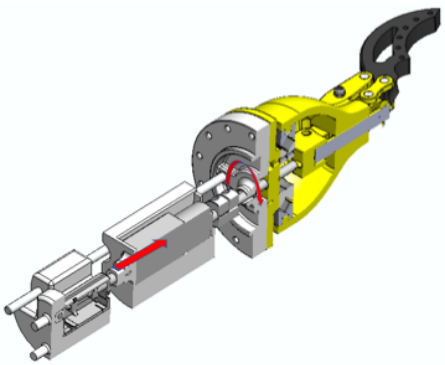

(b) Section of the shoulder mechanism

Figure 3.6: Setions of the two main components of the arm. Photo credit: PoliTOcean mechanical team

with a theoretically infinite possibility of rotation.

- In the **forearm** (3.6b), instead, there is a *NEMA8* that allows the gripper to rotate thanks to a 3D-printed fifth reel (see red rotating arrow). The stepper motor itself is instead allowed to be pushed back and forth thanks to a micro linear actuator (see red translating arrow), generating the closure or opening of the gripper. This system thus allows to simultaneously rotate and close/open the gripper.

In the shoulder, a shaft is transmitting the rotatory movement to the forearm, while in the forearm a shaft is transmitting both the rotary and translational movement to the gripper. One of the most important topic during the design of the arm was then the choice of the way to seal the shafts.
After various tests, custom seals made from a local factory have been used, that, according to our needs, have been built in *NBR* material for a roto-translating motion and with resistance up to a pressure of 10 bar with a low friction.

3.2.2 Chassis

The new chassis have been made with *HDPE* sheets,with their shapes obtained with CNC milling process.
The chassis is composed of four main components: one panel on the top,

one panel on the bottom and two lateral panels. The two lateral panels are connected to the top and the bottom panels using threaded inserts that allow to have a safer connection between parts. The threaded inserts need very large holes to be correctly installed, therefore it was necessary to use sheets with a thickness of 15 mm to maintain structural integrity.
The current shape of the plates has been chosen for several reasons: to minimize disturbances in the flow of thrusters, to reduce weight and to respect the dimensional constraints imposed by the manual (the length of the assembled chassis is smaller than 64 cm).
Moreover, a system with pins have been used in order to lock the electronic enclosure but allow it to rotate when unlocked. In this way it is possible to rotate the electronics housing, remove the acrylic tube and then have a comfortable access to the electronics, in case of maintenance.

Figure 3.7: Chassis with the electronics'enclosure. Photo credit: PoliTOcean mechanical team

3.2.3 Thrusters

In the previous R.O.V., only six thrusters were available and thus the configuration in Figure 2.3 has been adopted rather the one described in Figure 2.4. Anyway,on the new vehicle it has been chosen to adopt a configuration that has the advantages of both them. This means that four horizontal thrusters have been oriented with 45° angles to cover *yaw*, *surge* and *sway* and four horizontal thrusters have been used to implement *roll*, *pitch* and *heave* movements, as can be seen in Figure 3.8.

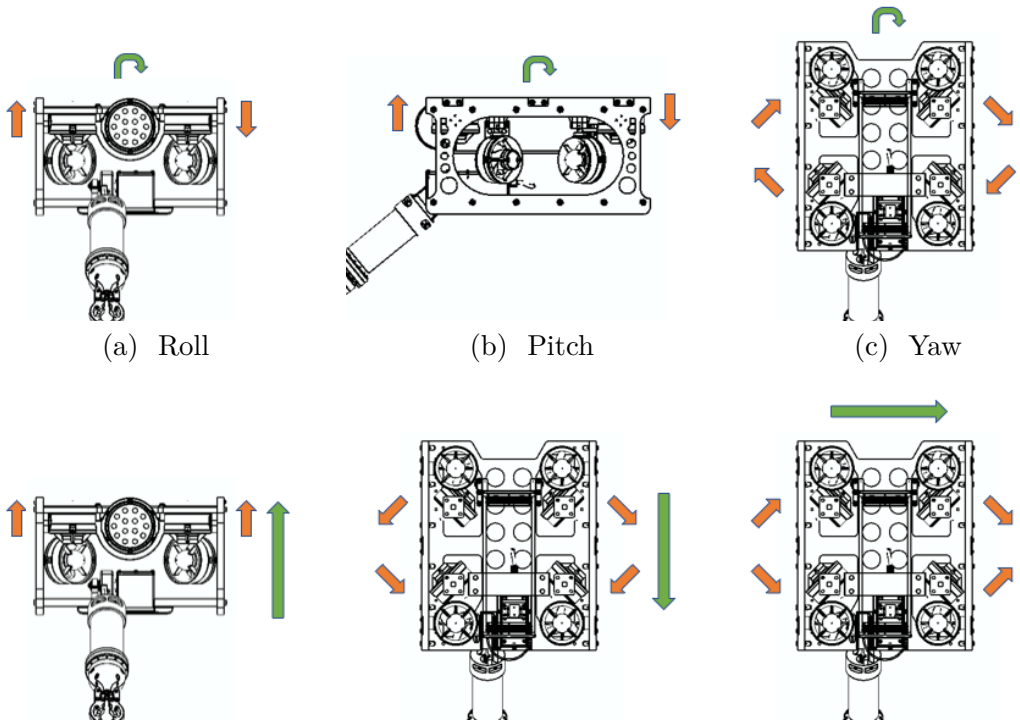

(a) Roll (b) Pitch (c) Yaw

(d) Heave (e) Surge (f) Sway

Figure 3.8: Motor piloting for the movements of *Nereo*.

This choice has been made for four main resons : power, reliability, control and future improvements. *Nereo* in facts, assuming a 12 V power supply, is able to generate in forward motion up to 11.5 kgf thrust (considering turbulance loss due to flux interferences) and 20 kgf in a upward motion at full power.
This solution of course implies an increase in the area, weigth and cost of both the electronic and mechanical aspects.

3.2.4 Mechanical assembly

Besides the mechanical arm, from a mechanical point of view, substantial changes have been made for the design of *Nereo*. The main one, that could be seen from Figure 3.9 are:

1. The **chassis** have been made out of four 15 mm thick *HDPE* sheets, with their shapes obtained with a *CNC* milling process.

2. A **ballast tank** have been added, in order to ensure a uniform buoyancy to the chassis. It is foldable, in order to easily access to the electronics enclosure and it has been made out of 3D-printed canisters filled with polyurethane foam.

3. The **8 motors** configuration have been necessary in order to allow the R.O.V. to have all the six degrees of freedom, in exchange for a loss of thrust in the horizontal plane due to the 45° degrees configuration of the four horizontal motors.

4. Two **cameras** were added: one on the dome of the electronic enclosure, provided with a micro-servo to tilt it and allow the pilot to increase the field of view (see Figure 3.14 for a better view), and another one oh the forearm of the robotic arm. This one was particularly useful in operations in which the pilot had to manipulate some objects, with the arm tilted in such a way that didn't allow the pilot to see the gripper with the main camera. An application of its usage can be found in the O.B.S. task.

Figure 3.9: Mechanical assembly of *Nereo*. Photo credit: PoliTOcean mechanical team

3.3 Electronics

As well as the mechanical aspects, the electronics needed some changes.
First of all, two camera signals had now to be sent to the surface, so a serial communication protocol was not enough anymore.
The number of motors to be managed increased, both for the increase on the number of thrusters of the R.O.V. and for the need to add the three motors for the robotic arm.
Thus, a single microcontroller architecture was not enough to manage the navigation control system, the video stream from the cameras and the commands and feedbacks coming from *Nereo* to the surface control station and viceversa.
This led us to split the design of the electronics in three main PCBs, that will be described in the next subsections, whose simplified diagram is reported in Figure 3.10.
Notice that, for sake of briefness, the architecture of the surface control station will not be analyzed, but it would be sufficient to say that is composed of a *Raspberry Pi* with some input and output peripherals (Joystick, Keyboard and a Monitor).

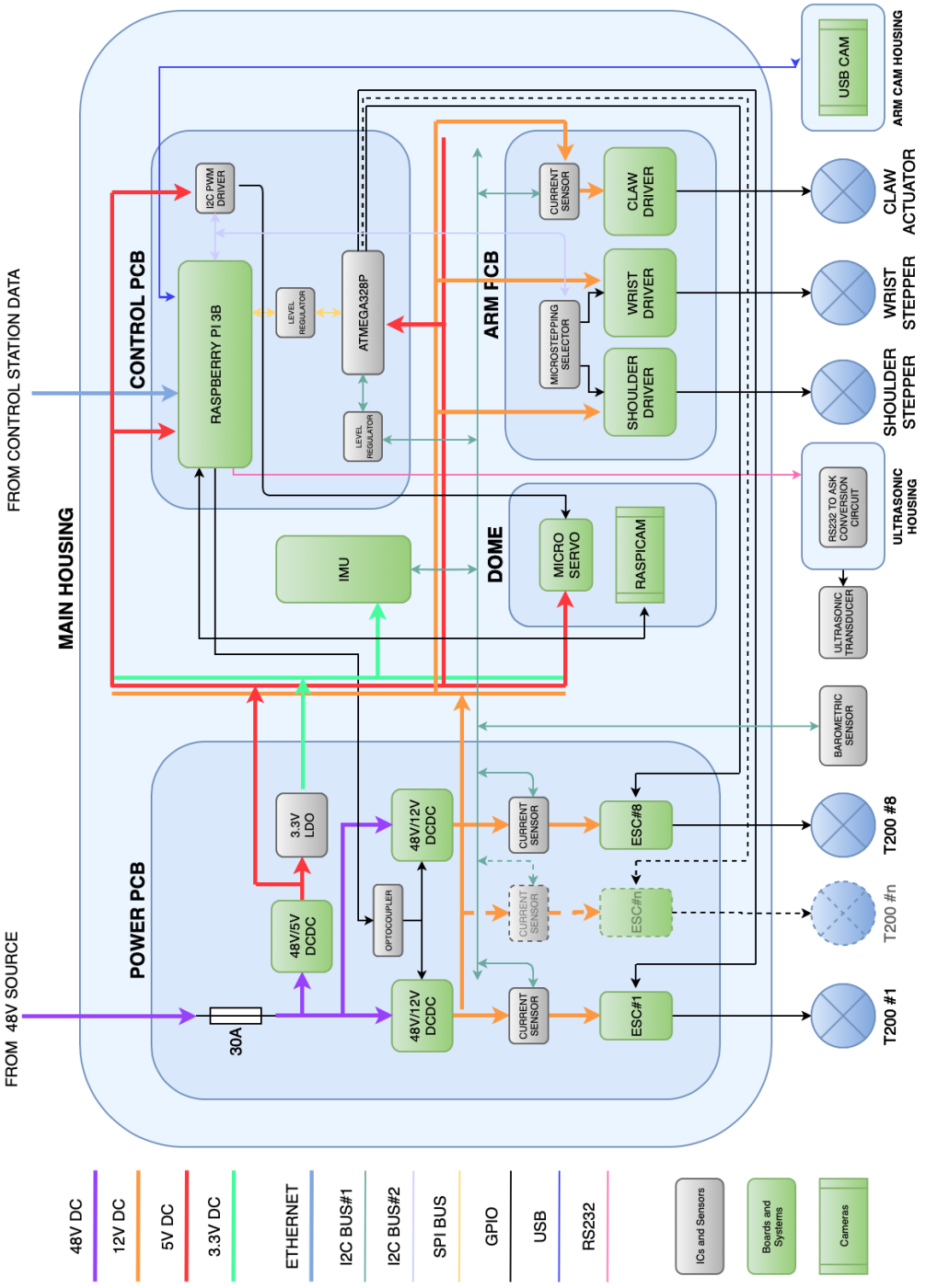

Figure 3.10: The *SID* of the *Nereo* electronic and electric system. Photo credit: PoliTOcean electronics team

3.3.1 Power PCB

Due to the complexity of *Nereo* with respect to the first prototype, it has been decided to assign the management of the eight thrusters to a single PCB.
As we can see in Figure 3.10, in the Power PCB section, 48V are coming from the surface to the R.O.V.: this voltage is a constraint as it is the power provided from the battery packs at the competition event. The 5V conversion is directly made by means of a 48/5V DC-DC converter and it is always enabled in order to supply all the logic components.
After that, it can be noticed that the couple of 48/12V DC-DC is enabled by a common optocoupler, controlled by the microprocessor on-board. This is a safety measure, took in order to avoid possible unwanted activation of both the R.O.V. thrusters and/or the robotic arm, possibly causing damage to the operators or to the system itself.
By means of an appropriate shunt resistor, an *INA220* current monitor is placed in series to each *ESC* that will control the thrusters. This is done since a single thruster could draw up to 25 A, so the microcontroller must menage each of them in order to not overcome a certain total current amount on the PCB.

3.3.2 Arm PCB

About the robotic arm, also here we decided to dedicate an own PCB, more of sake of modularity than power concern.
Two stepper motors are used to control the shoulder and wrist, controlled by means of two *Pololu DRV8825*. This drivers allows to select the microstepping factor, useful in case we want to reduce or increase the velocity of the steppers, for the same pulse clock. Since the driver is intended to do this manually by means or shortcircuiting or not some jumpers, an *ADG715* analog switch has been placed, so that the microstepping factor can be changed during its operation.
The claw (or gripper) is instead a linear actuator. It is controlled thanks to an *Pololu MAX14870* and also here an *INA220* is used, in order to possibly obtain the torque applied to the handled object as a direct proportionality of the current.

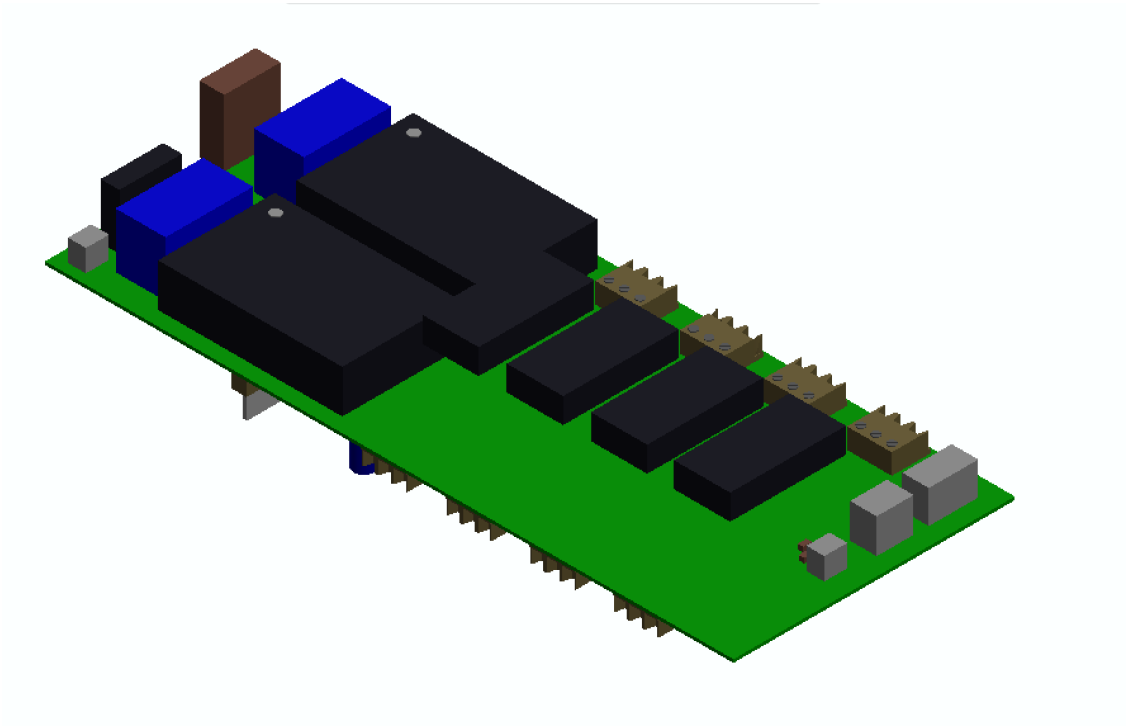

Figure 3.11: 3D rendering of the Power PCB. Photo credit: PoliTOcean electronics team

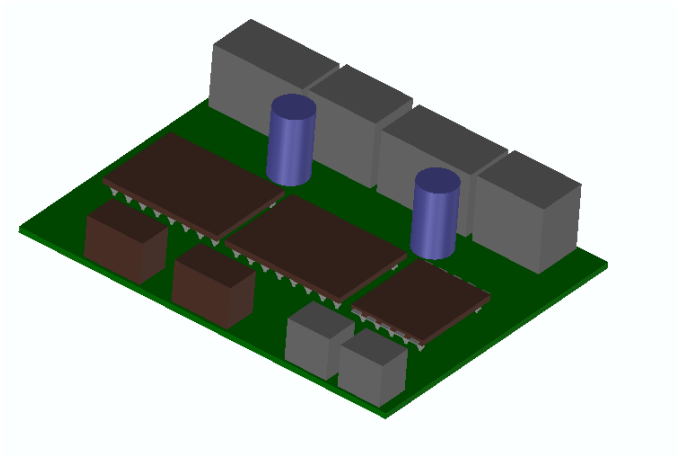

Figure 3.12: 3D rendering of the Arm PCB. Photo credit: PoliTOcean electronics team

3.3.3 Control PCB

The control PCB essentially let the microprocessor *Raspberry Pi* , the microcontroller *ATmega328P*, all the peripheral such as cameras and the boards previously described to communicate between each other. The *Raspberry* only is responsible for the communication to the surface, since it can easily communicate with the same microprocessor that can be found on the control station, thanks to the framework called *ROS*. The communication essentially carries the joystick command given from the pilot, and gives back some data such as the *IMU* ones and the cameras videostream.
The data coming from the surface is then processed and sent to the microcontroller, to which the navigation system and the piloting of the thrusters is entrusted, through an *SPI* bus. The *SPI* bus have been chosen since the same one can be exploited for the microcontroller flashing through the microcoprocessor, and thus from the surface through an *SSH* connection, without having to put hands on the R.O.V. once it has been sealed.
We can notice that two I^2C buses are used. The microcontroller, in fact, is the master communicating with the *IMU* and the current sensors, while the microprocessor in entrusted to communicate with those device whose timing is not that critical, such as the microstepping selection of the steppers and the PWM signal for the camera tilting.

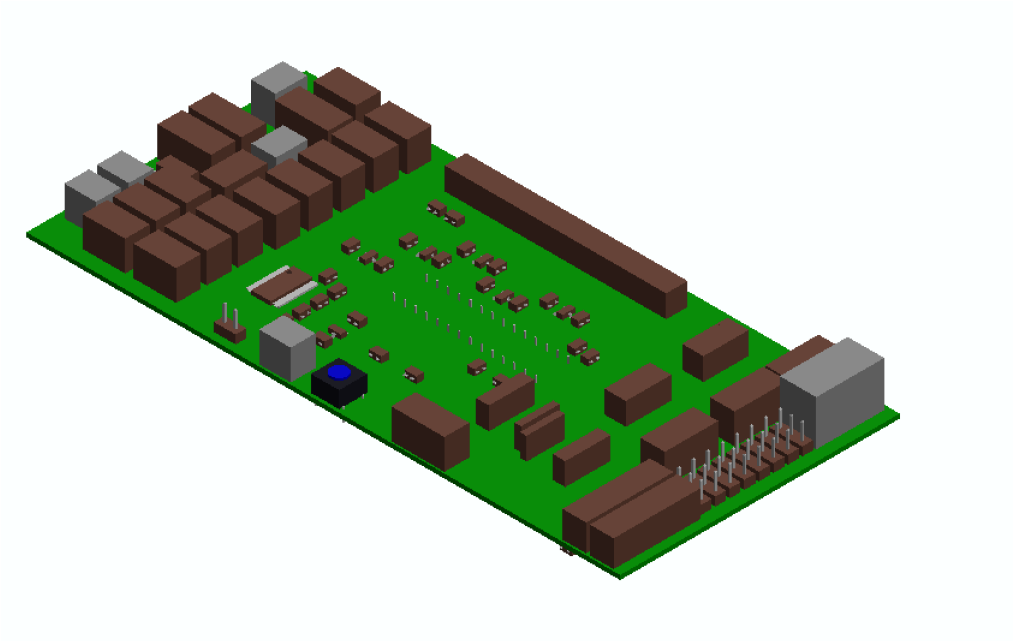

Figure 3.13: 3D rendering of the Control PCB. Photo credit: PoliTOcean electronics team

3.3.4 Electronics Assembly

In Figure 3.14 a photo of the electronic assembly can be seen. The three PCBs are held toghether by means of some 3D-printed PLA rings, so that the whole systems results a neat cylindrical shape to be easily inserted and removed from the main acrylic enclosure.
We can distinguish:

1. **Power PCB**, placed in the "bottom" of the cylinder and occupying almost the 50% of its volume

2. **Arm PCB**, placed near the penetrators

3. **Control PCB** with the *Raspberry Pi* placed on top of it

4. **Main camera** with the microservo for the tilting system

The *IMU* is not visible in the photo but it is placed near the center of the cylinder, under the Power PCB.

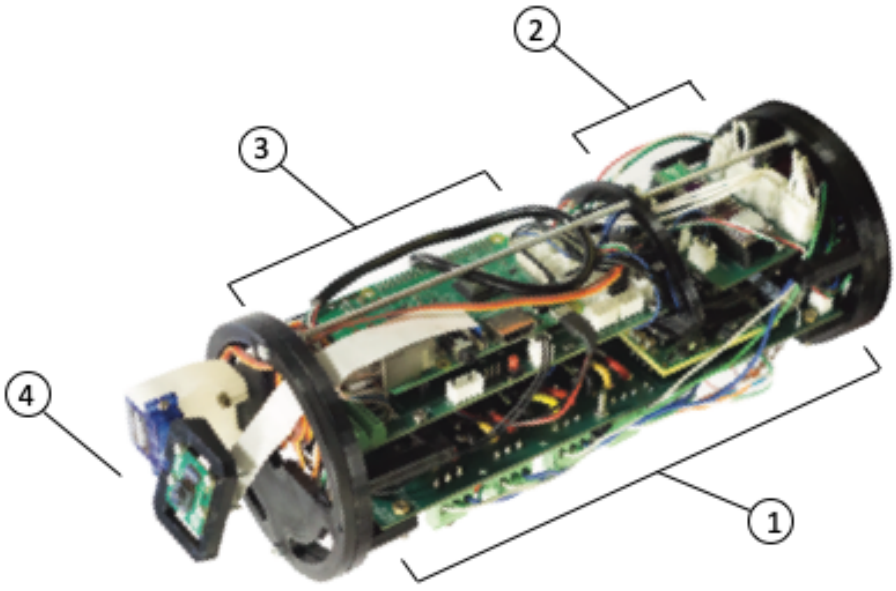

Figure 3.14: A photo of the elctronic assembly. Photo credit: PoliTOcean electronics team

3.4 Software

As said, for *Nereo* it has been decided to use a microprocessor for the control of the thrusters and navigation, and a microprocessor (*Raspberry Pi*) for the communication with the surface and other features.

3.4.1 ROS

The communication with the surface is based on *ROS* (Robotics Operating System) and there are two Raspberry boards: the main one is in the R.O.V. while the other is mounted on the control station in the surface, connected together through a network cable.
The main reasons that brought to choose *ROS* is its modularity, since it has been a great advantage for the development process and the system gains a significant scalability. Furthermore, this modularity allows to eventually include external developed nodes: as an example, the camera nodes are taken from the *ROS* libraries [6],while the other are custom.
Finally it has been decide to implement the scripts in Python instead of C++, because the last one needs to be compiled affecting the prototyping phase.
The terminal node is the *GUI*, executed on the control station on the surface, useful for the visualization of the data written in the *ROS* topics. It has been developed with the *PyQT* libraries [7] and contains a console text module to communicate with *ROS*, to display video streams, error messages and to send control signals.
Figure 3.15 represents a simplified architecture diagram of the *ROS* architecture.

3.4.2 ATmega

Regarding the microcontroller *ATmega*, it is responsible for the self-stabilization control algorithm: the navigation input data are taken from the joystick and the *Raspberry Pi* onboard is in charge of sending them to the *ATmega*. This algorithm is written to implement a purely proportional controller. Initially, it was designed as a PID controller, but it has been proven that for *Nereo*'s purposes a simply proportional one was enough.
A software saturation is also implemented to take into account the physical

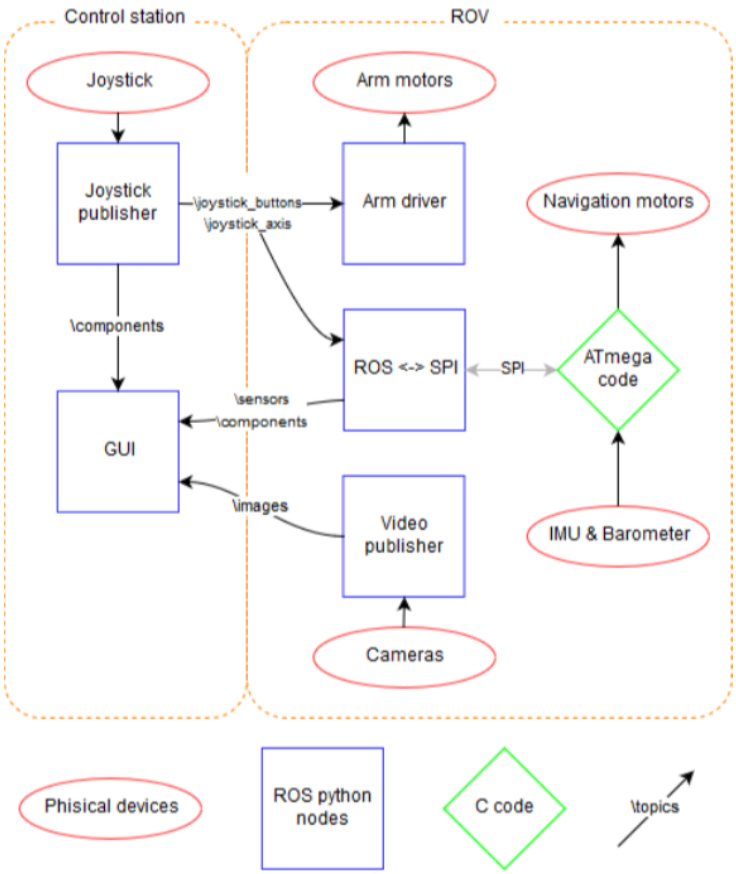

Figure 3.15: Flow chart of the ROS system. Photo credit: PoliTOcean Software team

limitation of the motors and to reduce the output current. Through the definition of a reference point and an error function the proportionality constant is found experimentally: in this way the attitude of the R.O.V. is correctly stabilized when the measured values are too different from the reference ones. To obtain the angle measurement, it has been initially used an atan2 function: this resulted in inaccurate results since it is an approximation unable to take into account all the necessary computation factors. For this reason, angles have been compute through the inversion of the rotation matrix [8]. A pressure sensor is used in order to automatically set the operative depth. In this way the pilot does not have to constantly take care of the horizontal thrusters, since the R.O.V will stop the *heave* movement maintaining the depth reached.

Figure 3.16 represents a simplified architecture diagram of the *ATmega* architecture.

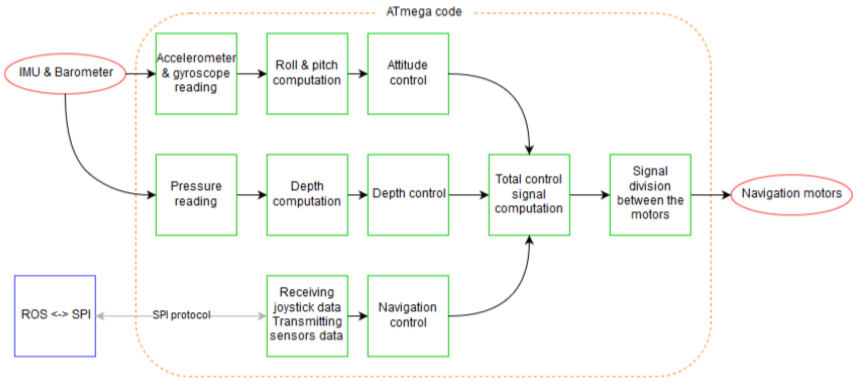

Figure 3.16: Flow chart of the ATmega navigation algorith. Photo credit: PoliTOcean Software team

3.5 Features

Also in this case, the maximum operative depth is 100 m, not only because of the acrylic tube but also for the arm shaft seals.

- 48V 30A power supply
- 26.5x39x59cm (HxWxL chassis only)
- 3 degrees of freedom (shoulder, wrist and gripper) 38cm long arm
- 23 kg in air without cable
- 100 m maximum theoretical depth
- 6 degrees of freedom
- Autostabilisation on the horizontal plane
- Auto depth with 10cm resolution

One thing worth to be noticed is that the communication between the microcontroller and the microprocessor is on 8 bit.
One information that is passed through this channel is the depth to which the pilot sets the R.O.V. operation. This implies that, assuming a resolution of 1 meter, the maximum depth from a purely computational point of view is 255 m, without adopting any stratedy.
Since some of the competition task required some depth measurements with a certain resolution, one decimal point has been added to this information in order to have 10cm of maximum error.
This implies that, at the moment, the maximum reachable depth with the autostabilization turned on is equal to 25.5 m.

Chapter 4

Serial to ultrasonic communication system

It can be noticed, in Figure 3.10 the presence of an ultrasonic conversion circuit. It has not intentionally been described since it will be done here in this chapter.

4.1 Competition needs

As explained in section 3.1, in the description of the Aircraft task, the debris have to be moved away, meaning that the liftbag must attach and then release them.
This implies that the pilot must have the possibility to trigger the releasing mechanism of the liftbag, such that the debris could be detached from it and fall in the seafloor.
Each team could choose which kind of releasing mechanism it wanted to implement, among:

- **Mechanical**: Any device that requires the ROV to physically push, pull, bump,turn, or manipulate part of the lift bag release to execute the release.
- **Magnetic**: Any device that uses a magnet in close proximity to a magnetic reed switch or other similar device to complete an electrical circuit that executes the release of the lift bag.
- **Wireless**: Any device that uses transmission of an electromagnetic signal that is received by the lift bag release and results in the release of the

lift bag release. Bluetooth, WiFi and other such devices are included in wireless release.

- **Acoustic**: Any device that transmits an acoustic pulse that is received by the lift bag release and results in the release of the lift bag.

The team decided to develop an acoustic mechanism, both because it was the one that allowed to gain more points in the competition and because it was an occasion to learn about underwater acoustic communications.
I personally accepted this challenge and took the responsibility on the design and the development of the electronic communication system.

4.1.1 Mechanical design of the liftbag

About the mechanical part, the liftbag has been designed so that the pilot can easily both attach it to the debris and detach it without having to perform any particular movement. The idea has been to use a system like in Figure 4.1. A servo motor is used in order to pull a pin that is holding an hook, to which the debris are attached.
In this way, the pilot can easily attach the debris without having to activate any mechanism. Then, once they are attached and the liftbag has been inflated, the ultrasonic system on the R.O.V would send a triggering signal which will be interpreted from the electronics inside the liftbag in order to let the servomotor to move, causing the debris to fall down together with the hook.

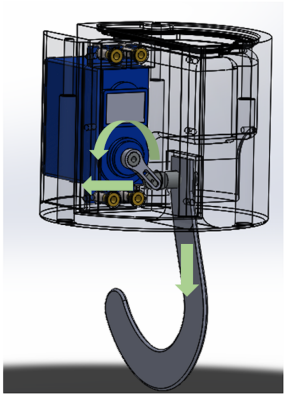

Figure 4.1: The liftbag releasing mechanism. Photo credit: PoliTOcean mechanical team

4.2 Concept

At the moment, there are no cheap solutions on the market intended to set up a *simplex* communication for a short range underwater communication system.
The competition manual required that the acoustic signal must have been a coded one in order to avoid possible errors due to noise inside the pool.
It has been decided to use an A.S.K. (Amplitude Shift Keying) modulation since it was particularly easy to be implemented [9] from an hardware point of view, as can be seen in the conceptual scheme in Figure 4.2.

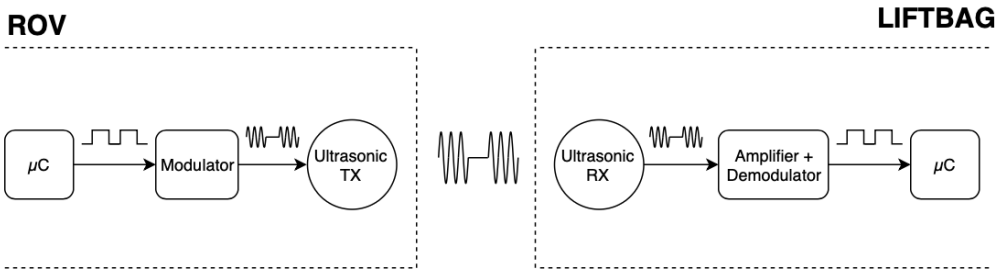

Figure 4.2: Conceptual scheme of the ultrasonic triggering system

In particular, the modulator may only consists in an astable multivibrator, turned on and off by the microcontroller. On the other side, the demodulator may consists in an amplification stadium plus some kind of decoder that must detect the envelope of the A.S.K signal and make it compatible to be read from a microcontroller.
Now, if we let the microcontroller on the R.O.V. side to pilot the multivibrator directly with a serial communication protocol, the liftbag microcontroller would then receive the same serial signal, making the modulation and demodulation transparent to the programmer.

4.2.1 Sensor choice

The underwater ultrasonic receivers and/or transmitters for data and positioning systems are mainly found in the range of 10 to 100kHz. Three cheap sensors (Figure 4.3) with similar characteristics were selected from the market, all with a center frequency of 40 kHz because of their easier availability. We will call the *a*, *b* and *c*.
The difference between *a* and the other two is that it is not waterproof and

cannot be used in the water as it is, so it has simply been used as a reference for measurement comparisons.

(a) (b) (c)

Figure 4.3: The three available pairs of ultrasonic transmitter and receiver

First of all, a simple test of all the three pairs has been made in the air at a distance of 10 cm. A 9V 40kHz square wave has been applied to the transmitter, measuring the peak-to-peak voltage value on every possible receiver.

Pair (TX-RX)	**RX voltage (mV)**
a-a	**1100**
a-b	144
a-c	160
b-a	400
b-b	**70**
b-c	60
c-a	440
c-b	40
c-c	**24**

Table 4.1: Measured voltages on each combination of transmitter and receiver

It goes that the highest measured voltage on the receiver is the one on the first pair, since the acoustic waves produced by the membrane do not encounter any particular obstacle as the transducer is not enclosed by any waterproof case.

4.3 First prototype

The first practical approach of the modulating and modulating circuit consists in a transmitting device to be carried with the R.O.V, sending the triggering signal through the *RS-232* standard.
A receiving PCB to be embedded into the liftbag, is then receiving the signal and, if it is the opening command, activates the releasing mechanism through the servo motor.

4.3.1 Schemes

Here the circuits scheme will be described reporting the most significant measurements on the corresponding PCB.
The measurements have been taken in the air for sake of simpicity, by positioning the two modules (RX and TX) at a distance of 10 cm with the transducer couple a-a. Each module was powered with a 9V alkaline battery.

Transmitting circuit

Starting from the transmitting circuit in Figure 4.4, from left to right, it can be noticed the high side switch for the reset of the *NE555* [10] oscillator, which is what actually allows the A.S.K. modulation, since it is configured in such a way that when it is ON is producing a square wave of 40 kHz on its output. This means that when the *RS-232* line is high, the *RST* pin goes high as well and the oscillator is enabled (since the reset is active low).
The trimmer *R6* is in fact used to center this precise frequency.
The output of the oscillator, at this point, is piloting the NPN BJT that lets the transducer to produce the wave.

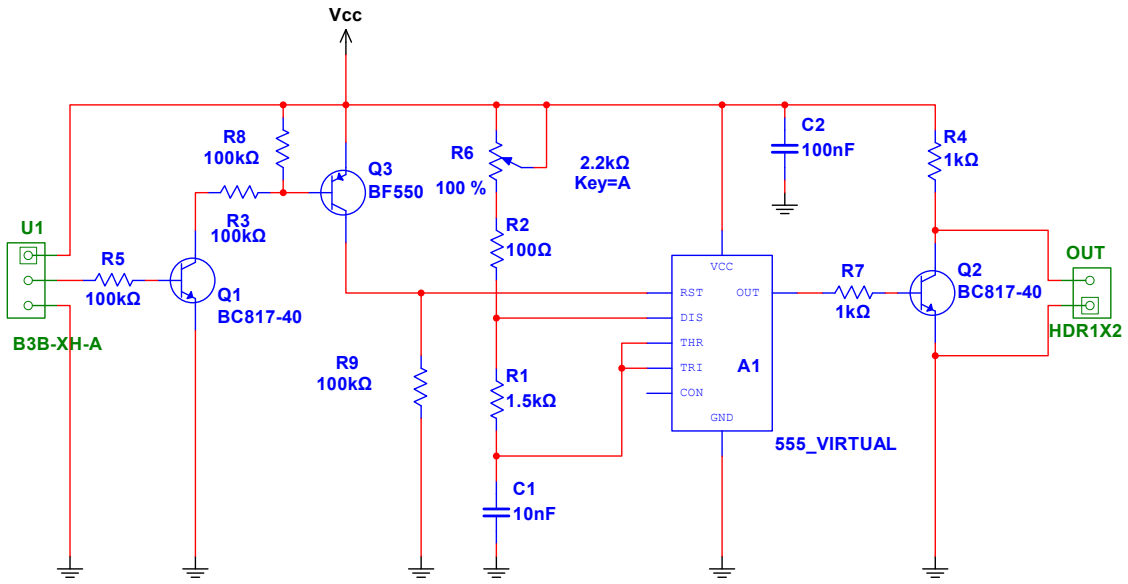

Figure 4.4: The first version of the transmitting circuit scheme

In Figure 4.5, the yellow trace *C1* represents the serial character *'A'* sent from the microcontroller to the input of the transmitting circuit every 10ms (note that the line is normally high), while the blue trace *C3* is the voltage applied to the transducer representing an A.S.K. modulation of the original message.
The trace *Z4* is instead a zoom of the trace *C3* to check whether the frequency is at 40 kHz.

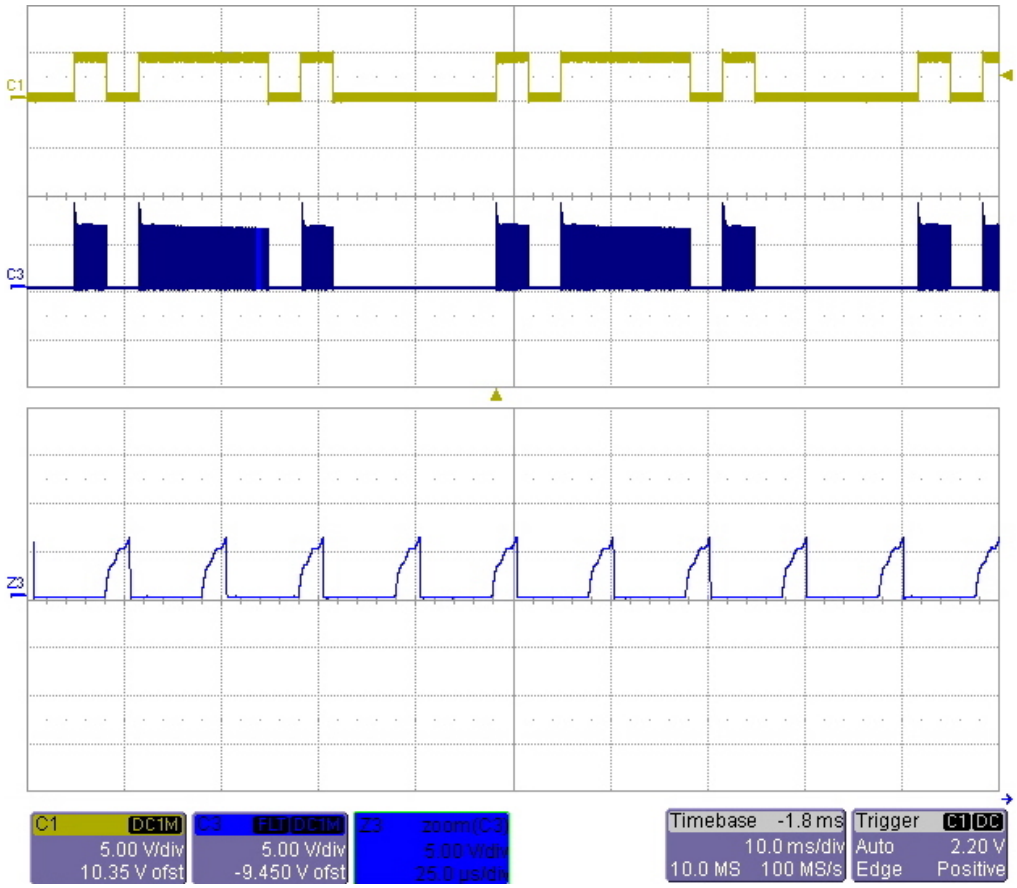

Figure 4.5: Measurements of the transmitting circuit

Receiving circuit

The other PCB, to be placed inside the liftbag, is composed as said in Figure 4.2 by an analog part that acts as amplifier and demodulator, and by a digital part that receives the demodulated signal and acts on the output peripherals. The analog part is represented in Figure 4.6.

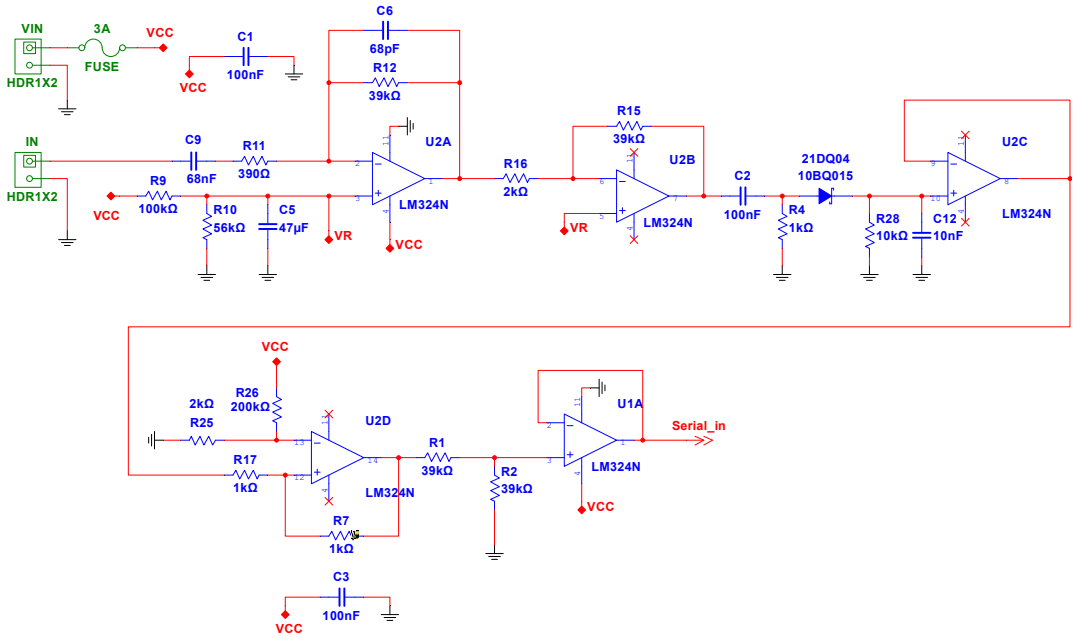

Figure 4.6: First scheme of the analog part of the receiving circuit

Starting from the left to the right, at the input of the connector *"IN"* the modulated acoustic signal is producing an electric signal of about 1 V_{pp} and it can be seen in Figure 4.7.
Again, the trace *C1* represents the message sent by the transmitting microcontroller, while the trace *C3* here represents the voltage on the receiving ultrasonic transducer. *Z3* is also is this case a zoom of the trace *C3*, still confirmed to be 40kHz. The first operational amplifier acts as a band pass filter thanks to the capacitors *C6* and *C9* and it is biased with the resistors *R9* and *R10* in order to maximize the output dynamic range, with a gain equal to 100. Its output can be seen on Figure 4.8.

The second amplifier has a lower gain and the envelope of its AC output (capacitor *C2* removes the DC component) is detected thanks to the diode and the *RC* circuit composed by *R28* and *C12*.
The envelope now needs to be transformed into a TTL compatible signal, and this is accomplished thanks to the non-inverting threshold comparator with hysteresis made with the fourth operational amplifier.
A voltage divider is made with the resistors *R1* and *R2* in order to translate the level from 9V to 5V. A voltage follower is placed before the comparator and after the voltage divider,in order to decouple the impedances with the remaining parts of the circuit.

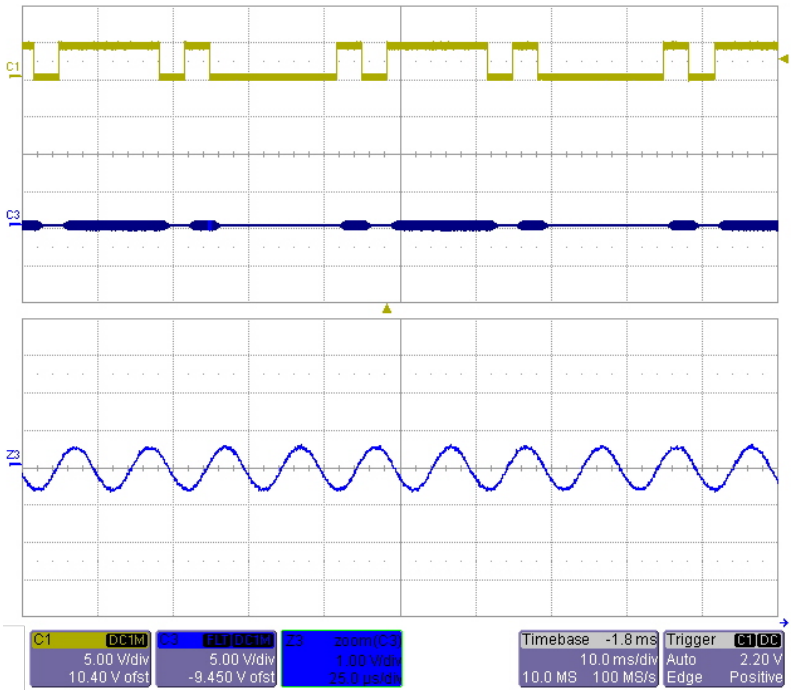

Figure 4.7: Measurement on the receiving transducer

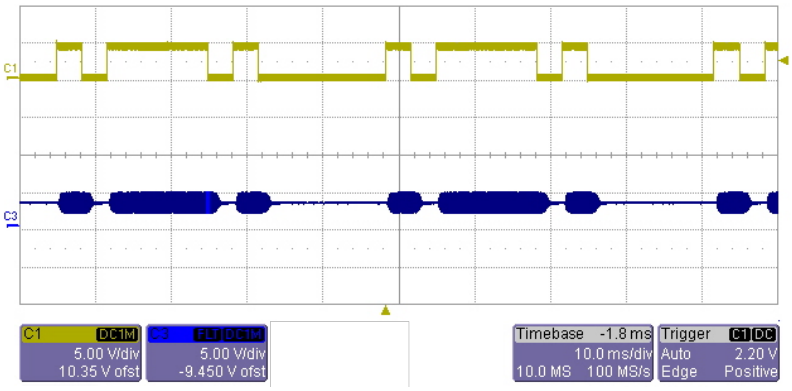

Figure 4.8: Output of the first operational amplifier

The final output can now be read by the serial pin of the receving microcontroller, and it is represented in Figure 4.9. Trace *C1*, as before, represents the *RS-232* message sent by the transmitting microcontroller, while *C3* now represents the demodulated message to be read by the receiving microcontroller.

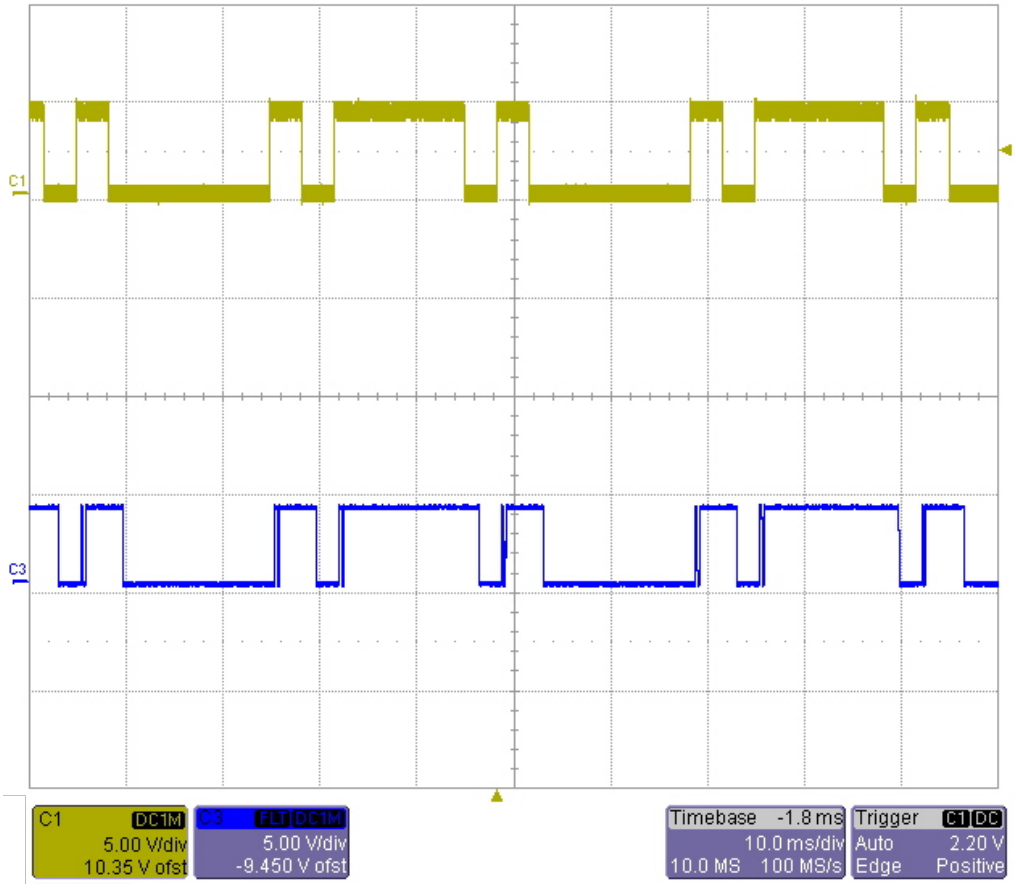

Figure 4.9: Output of the demodulator

Figure 4.10 shows the digital part of the receiving circuit.
An *ATmega328P* has been used to read the serial message and to act on the servo.

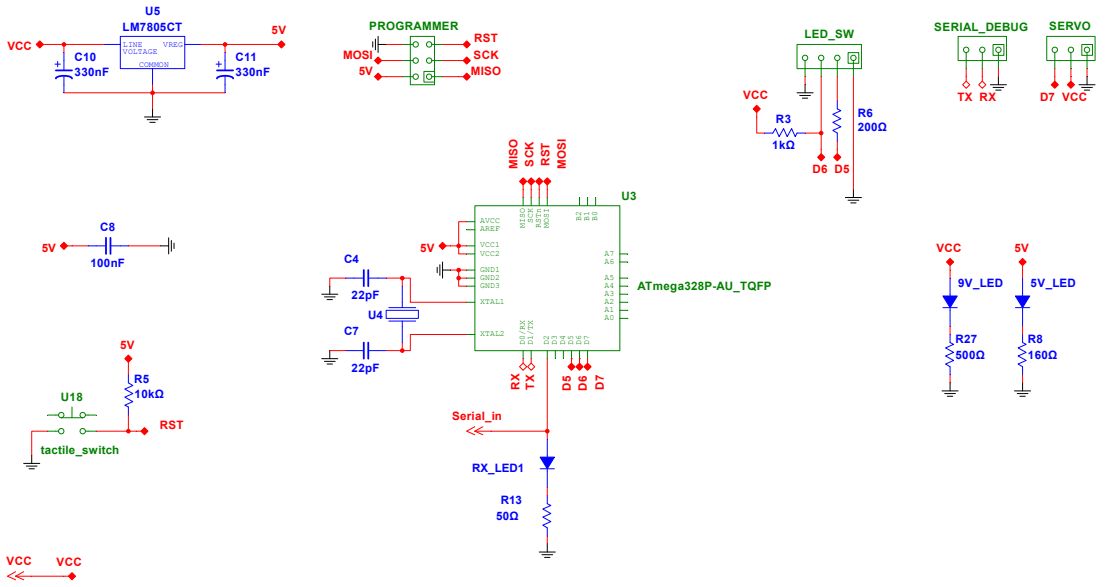

Figure 4.10: First scheme of the digital part of the receiving circuit

Note that the serial output of the analog stadium goes to a GPIO instead of the hardware *RX* pin. This is done because a library is used in the microcontroller code, in order to create a "Software" serial and leave the hardware serial pins for debuggin purposes.
The various connectors are used for:

- Programmer: access to the SPI pins to flash the microcontroller code
- LED_SW: The first two pins (left to right) are used to read a magnetic switch. It has been decided, in fact, to use a reed switch in case the ultrasonic system would not work. Thus, the resistor *R3* acts as a pull-up for the magnetic sensor while *R6* is placed in case we want to embed a led into the liftbag, usefull to show to the pilot the correct reception of the serial message
- Serial_debug: used to have access to the hardware TX and RX pins of the microcontroller
- Servo: used to attach the servomotor that is piloted in *PWM*

4.3.2 Implementation and PCBs

Receiver

A rendering of the whole liftbag is in 4.11a. As can be seen it is composed, from the top to the bottom, by:

- A bag in which the R.O.V. inflates the air by means of a small plastic pipe
- A central body in which the 9V battery is hosted, separately from the receiving PCB
- A cylinder in which the ultrasonic transducer is sealed and inside which the receiving PCB is hosted (see 4.11b)

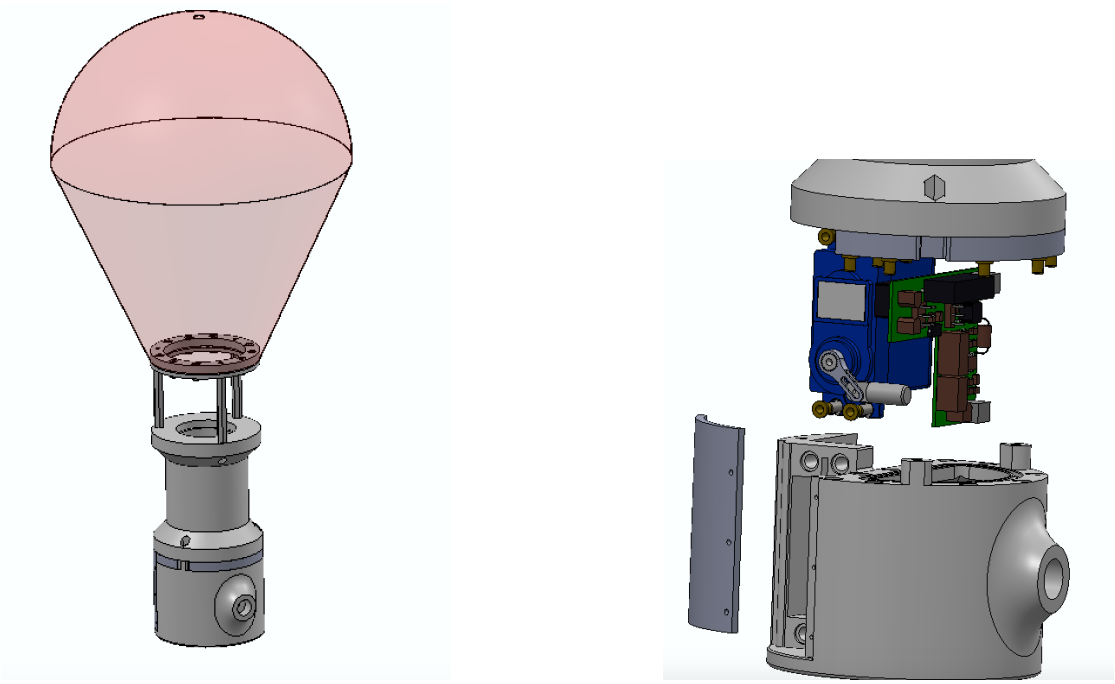

(a) (b)

Figure 4.11: Assembly of the liftbag and exploded view of the respective releasing mechanism. Photo credit: PoliTOcean mechanical team

Transmitter

The transmitting system, as said, has been placed into the R.O.V. as a separate device.
It is worth to say that a first approach was to create an housing with a classic non-waterproof sensor, with a thin plastic membrane to be placed in front of it such that it could propagate the ultrasonic vibrations on the water. This system can be seen in Figure 4.12.
In order to work properly from a theoretical point of view, the inside of this housing should have been filled with distilled water or other non-conductive liquids: in this way the density of the propagation medium would have been constant.

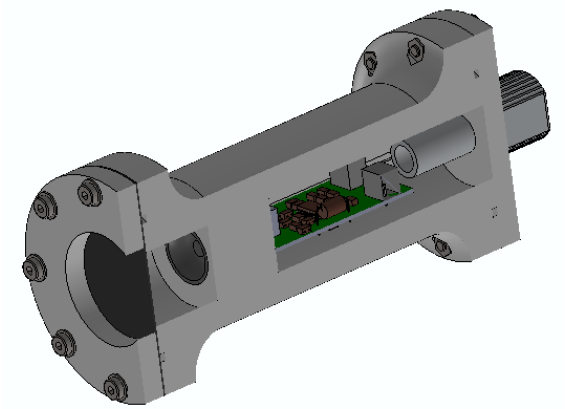

Figure 4.12: Section of the first transmitting system. Photo credit: PoliTOcean mechanical team

Anyway, it has been experimentally founded that this system does not work, mainly because of the small dimensions of the transducer whose waves are not able to let the membrane to vibrate.
As a solution, the ultrasonic transducer is sealed to the case as in Figure 4.13, being in direct contact with the water and reducing the overall dimensions as well.

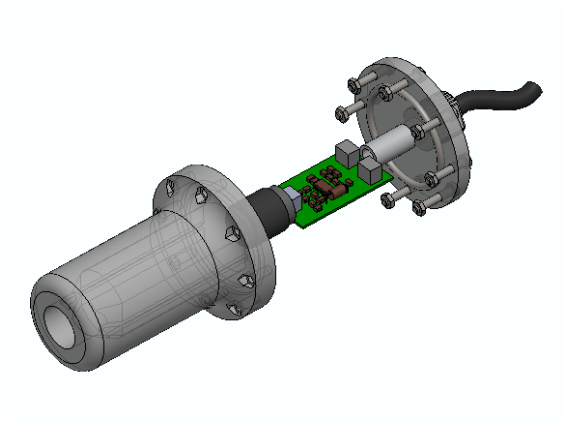

Figure 4.13: Exploded view of the final transmitting system. Photo credit: PoliTOcean mechanical team

The previously mentioned device called "Ultrasonic housing",in Figure 2.7, can now be fully understood as it represents what has just been described. It is connected to the main R.O.V. electronic enclosure through a cable that provides the powering (batteries where only used in the transmitting circuit for sake of simplicity) and the serial message.

A photo of the transmitting and receiving PCBs is instead in Figure 4.14.

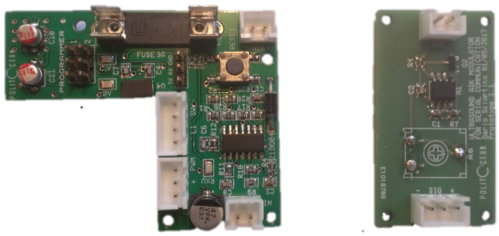

Figure 4.14: Receiving and transmitting PCBs (left to right)

4.3.3 Results

Maximum distances in the air

The previous system has been tested in the air with every possible pair of the available ultrasonic transducers.
To compare the configurations, the TX and RX modules have been distanced along a rectilinear path, until the message on the receiver was not correctly received anymore.

Pair (TX-RX)	Max distance (cm)
a-a	**70**
a-b	23
a-c	24
b-a	25
b-b	**2.5**
b-c	4
c-a	25
c-b	2
c-c	**4.5**

Table 4.2: Maximum working distances of the modules with the respective pairs of transmitter and receiver

Taking into account Table 4.1 with the voltage values of the couples, it is reasonable to see in Table 4.3 that the maximum distance covered by the couple *a-a* is at least one order of magnitude greater with respect to the couples *b-b* and *c-c*.

Drawbacks

The receiving system, as it is, suffers too many problems in the analog part, especially in the threshold comparator that is too dependent on the voltage and resistor values, that are difficult to control.

4.4 Second prototype

A second version of the system has been setup, mainly due to the drawbacks described before.
The main change consists in the usage of a tone decoder that would act as demodulator and bandpass filter at the same time. [11]

4.4.1 Schemes

Transmitting circuit

The transmitting circuit has basically been left unchanged, except for little improvements such as the addition of LEDs to signal the transmission of data and the presence of power.

Receiving circuit

The analog part of the receiving circuit instead, drastically changed thanks to the tone decoder *LMC567*. [12]

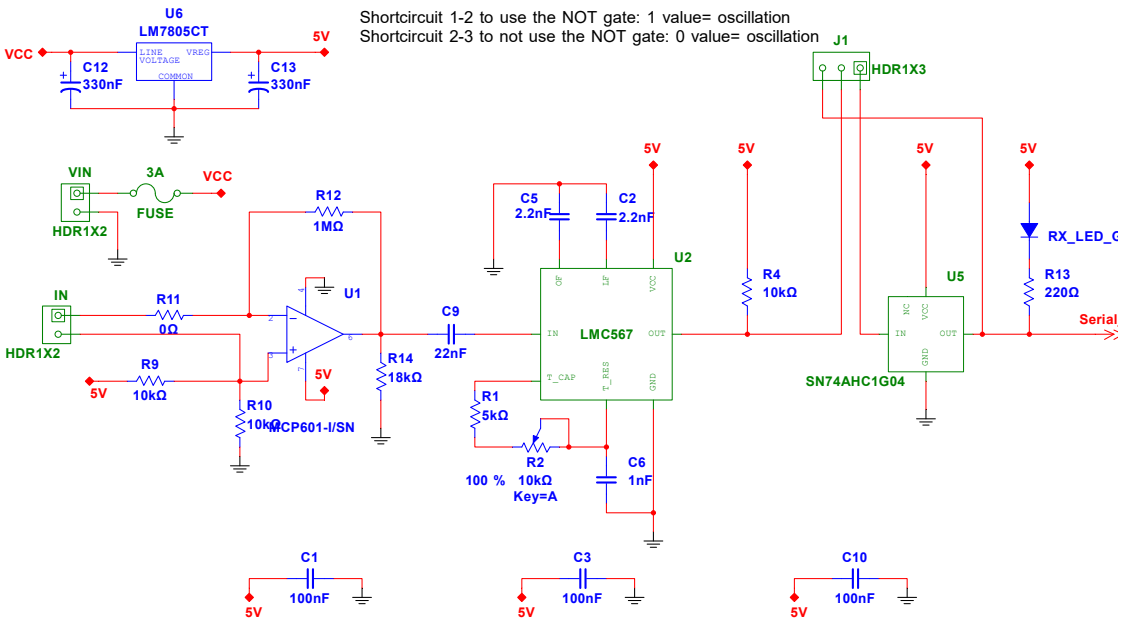

Figure 4.15: Second scheme of the analog part of the receiving circuit

Even if the input threshold of the tone decoder is 45 mV_{rms} if $V_s = 9V$, thus enough under particular conditions and sensors, an operational amplifier has still been used in order to have a better signal. The Microchip *MCP601* [13] have been chosen thanks to its low input noise voltage density that is, at 40 kHz, around 24 $nV/\sqrt{Hz}$.
About the tone decoder, the inside phase detector and VCO form a phase-locked loop (PLL) which locks to an input signal frequency which is within the control range of the VCO. When the PLL is locked and the input signal amplitude exceeds an internally pre-set threshold, a switch to ground is activated on the output pin.
As VCO frequency (F_{osc}) runs at twice the frequency of the input tone (specific for LM**C**567), the desired input detection frequency can be defined as:

$$F_{input} = 2F_{osc} \tag{4.1}$$

The central frequency of the oscillator is set by timing capacitor and resistor as follows:

$$R_1 = \frac{1}{2.8F_{input}C_6} \tag{4.2}$$

The detection bandwidth is represented as a percentage of F_{osc} and it can be approximated as a function of F_{osc} x C_2 following the behavior indicated in Figure 4.16

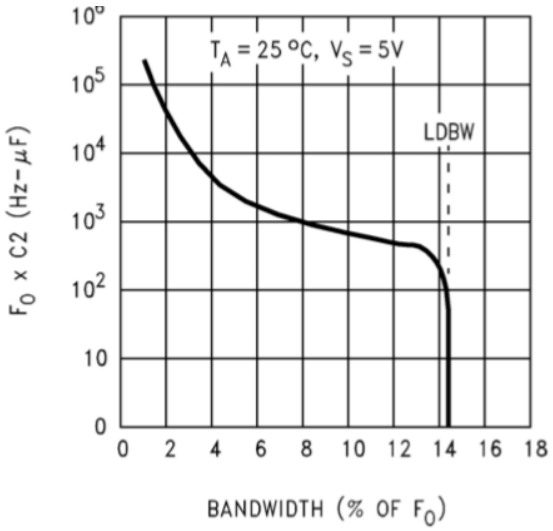

Figure 4.16: Bandwidth with respect to the F_{osc} and C_2 values

Recalling Equation 4.2, if we choose F_{input} to be 40 kHz and C_6 to be 1 nF, we obtain that R_1 must to be 8.9kΩ.

Thus, R_1 have been chosen to be equal to 5 kΩ to be added in series of a trimmer of 10 kΩ that would have allowed to lock the resonance frequency of the transducer with the best precision.
The logic inverter *U5* allows the possibility to invert the received signal through the jumper connections on *J1*. This feature was meant to invert the logic of the transmission, but was actually not used as this can be done in the software thanks to the library properties.
Figure 4.17 shows the digital part of the new receiving circuit, without any change except for an LED.

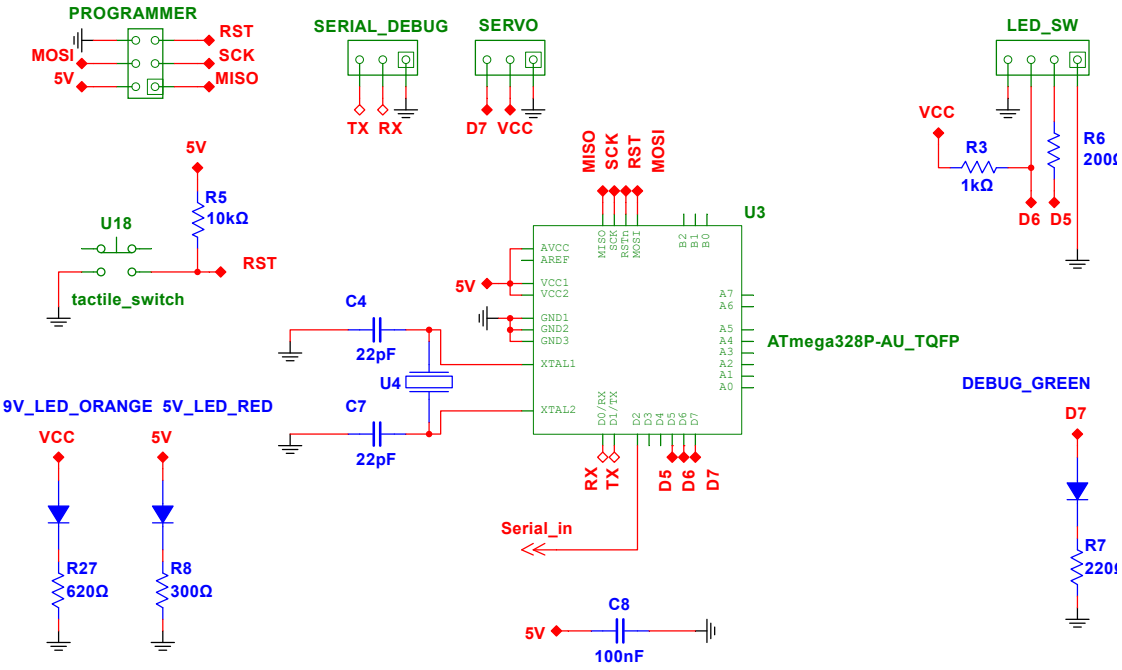

Figure 4.17: Second scheme of the digital part of the receiving circuit

4.4.2 Results

Maximum distances in the air

Again, a test of the maximum distance in the air have been done, this time with the new demodulation circuit.

Pair (TX-RX)	Max distance (cm)
a-a	**135**
a-b	45
a-c	59
b-a	25
b-b	**13**
b-c	25
c-a	35
c-b	4
c-c	**17**

Table 4.3: Maximum working distances of the modules with the respective pairs of transmitter and receiver

In general, the maximum distances doubled. This may easily be due to the new demodulation system that as explained before, is more sensitive.

Maximum speeds in water

The wet tests of the second prototype have been only made with the couple *c-c*, as it represents a worst case scenario in terms of signal strength and also because of their mechanical predisposition to be attached to a solid structure. In fact, two 3D-printed PLA supports have been designed in order to neatly attach the sensors and position them underwater in an easier way.
The wet tests have been done in a plastic box of about 40x20 cm, with a water level of 30 cm and again with the sensors at a distance of 10 cm as we can see in Figure 4.18.

Figure 4.18: Setup of the system

An example of the resulting waves can be seen in Figure 4.19. Again, the blue trace is the sent *RS-232* signal standing for an *'A'*, the green wave is the AC voltage read at the output of the amplification stadium, while the yellow one is the demodulated signal that is read by the receiver's microcontroller.

It is reasonable and also known [14], that the acoustic waves on the receiver are not only the direct ones but the superimposition of many reflections due to different paths that the wave takes.
This phenomenom is called multipath, and is the main reason of the low data rates of the underwater acoustic communications. In fact, as we increase the bit rate, the number of error will increase as well due to the *ISI* (Intersymbol interference) caused by the multipath effect [15].
To evaluate this kind of behaviour on the system, a test has been made,

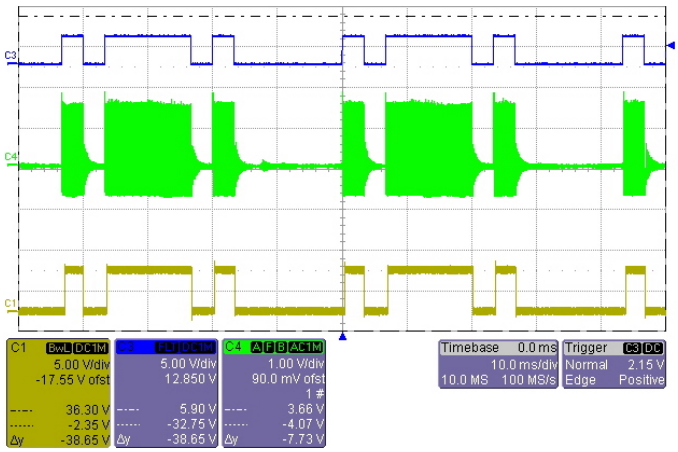

Figure 4.19: Example of waves with the character *'A'*

consisting in transmitting a certain number of characters at different speeds, in order to evaluate the number of detected errors.
In particular, the transmitter sends 50 equal characters (*'A'*) at intervals of 1 ms and the receiver, in a window of time of 3 s, counts how many correct characters have arrived.
This test have been done starting from a baudrate of 300, going up to 3000 with intervals of 300 baud.
The results can be seen in Figure 4.20 and, as expected, the percentage of success decreases as the baudrate is increased.

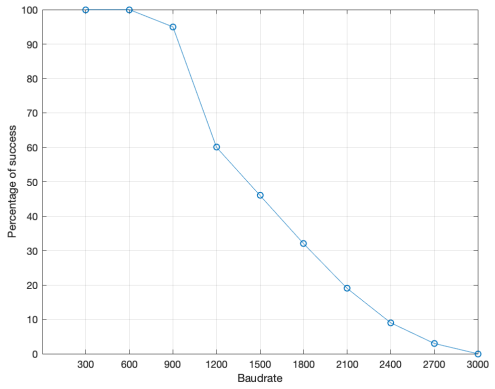

Figure 4.20: Degradation of the communication with respect to the baudrate

Chapter 5

Conclusions

Team PoliTOcean

The team successfully achieved all the main proposed targets, with a constant work always equally distributed among all the members.
The construction of the first prototype served as a springboard to understand, at the beginning, at least the basis of the R.O.V. world. This should be intended as learning nomenclature, knowing the R.O.V.'s configurations and uses with an understanding of their typical components.
This allowed us to develop a certain knowledge, sufficient to inspire and involve other students before the construction of the second vehicle.
The second R.O.V., in fact, implied many changes and additional features with respect to the previous one, needing more people to work on it.
Considering that the main purpose of the team was to introduce inside the university the topic of underwater robotics, it is clear that the team did a lot more as it has been selected to compete to the *MATE R.O.V.* Competition at its first attempt.
The participation is in fact not guaranteed, and needs a selection process between hundreds of teams starting with the submission, at least one month before the event, of a video of the R.O.V. performing some of the competition's tasks.
It has to be said that the competition didn't end very well, as during the test the afternoon before the competition the dome of the electronics enclosure popped due to the excessive heat. This caused the water to flood the PCBs, making several shortcircuits to components that required too much time to be substituted.
Anyway, the competition reserved us many opportunities to show the project,

receive many compliments for the design and talk with other students as passionate as us about this world.

Ultrasonic underwater communication system

The system, considering its cheap and easily available components, resulted to be an effective solution for the transmission in the air, for distances in the order of meters.
Unfortunately, even if acoustic waves better propagate in water with respect to the air, more problems arise as seen in the previous chapters.
Furthermore, the waterproof ultrasonic transducer that have been used, do not result to be suited for an underwater transmission system usage, but do work for distances in the order of some centimeters, that is more than enough for the mission purpose.
Anyway more appropriate, but expensive, sensors are available on the market and are intended for this kind of usage, allowing to extend the transmission range.

Appendix A

A.1 Penetrators

A penetrator is a simple solution to waterproofing cables that have to go inside an enclosure. It's basically a bolt with a hole that the cable can be glued into, in order to provide a waterproof connection through watertight enclosures, boxes, panels, etc. The bolt is usually provided with an *O-ring* that ensures the waterproofing, as can be seen in A.1a.

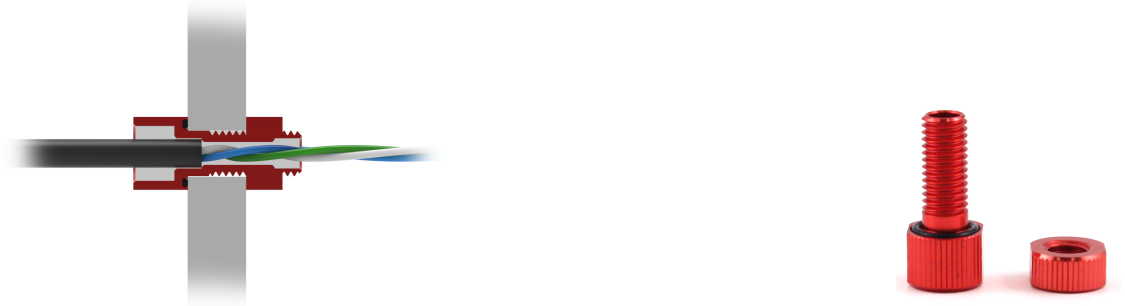

(a) Section of a cable penetrator

(b) Penetrator with its *O-ring* and the nut

Figure A.1: Penetrators by *Bluerobotics*

The bolt has then to be tighten by a nut, as in A.1b.

A.2 ESC

It is an achronym that stands for Electric Speed Control. Since in the reported case the motors are brushless, brushless *ESC*s are used, circuits that basically create three-phase AC power for the motor.

A simplified scheme of the circuit controlling a brushless motor is in Figure A.2.

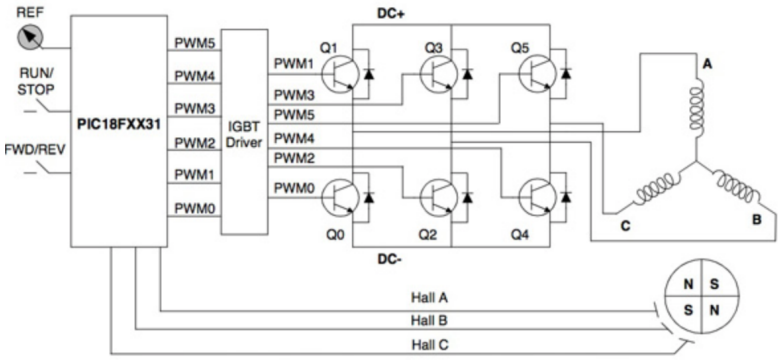

Figure A.2: Simplified scheme of the control of and ESC. Photo credit: see [16]

A.3 Liftbag

A liftbag, or *lifting bag*, is an air-tight device used in order to move or lift heavy objects underwater.
They come in different shapes and dimensions, depending on the weigth of the object and on their air inflation system.

Figure A.3: Israeli Navy Underwater Missions Unit transfers equipment using lifting-bags

Bibliography

[1] R. Capocci, G. Dooly, E. Omerdic, J. Coleman, T. Newe, D.J.F. Toal, *Inspection-Class Remotely Operated Vehicles—A Review*, 2017

[2] https://www.bluerobotics.com/new-products-aluminum-tubes/

[3] https://www.bluerobotics.com/pressure-testing-3000m-depth/

[4] https://plot.ly/create/?fid=rjehangir:96/

[5] F. Bonicelli, *Progetto PoliTOcean*, pp. 4-8, 2018

[6] http://wiki.ros.org/videostreamopencv

[7] https://wiki.python.org/moin/PyQt

[8] F. Bonicelli, *Progetto PoliTOcean*, pp. 6 section "Secondo metodo", 2018

[9] X. Lurton, *An introduction to Underwater Acoustics - Principles and applications*, Second edition, pp. 241-244, 2008

[10] http://www.ti.com/lit/ds/symlink/ne555.pdf

[11] P. Yichao, C. Waylon, *Mechatronic Football Ultrasonic Positioning System*, pp. 9-11, 2012

[12] http://www.ti.com/lit/ds/symlink/lmc567.pdf

[13] http://ww1.microchip.com/downloads/en/devicedoc/21314g.pdf

[14] A. Boayue, *Characterization of Underwater Acoustic Communication Channels - Statistical Characteristics of the Underwater Multipath Channnels*, pp. 12-13, 2013

[15] J. Kim, J. Park, M. Bae, K. Park, J.R. Yoon, *Effect of frequency dependent multipath fading on non-coherent underwater communication system*, 2016

[16] https://www.digikey.it/it/articles/techzone/2013/mar/an-introduction-to-brushless-dc-motor-control